Check for updates

Received: 4 September 2023 | Revised: 4 January 2024 | Accepted: 8 January 2024

DOI: 10.1111/prd.12551

Periodontology 2000 WILEY

REVIEW ARTICLE

The development of non-resorbable bone allografts: Biological background and clinical perspectives

Richard J. Miron[1] | Masako Fujioka-Kobayashi[2] | Michael A. Pikos[3] | Toshiaki Nakamura[4] | Takatomo Imafuji[4] | Yufeng Zhang[5] | Yukiya Shinohara[4] | Anton Sculean[1] | Yoshinori Shirakata[4]

[1]Department of Periodontology, University of Bern, Bern, Switzerland

[2]Department of Oral and Maxillofacial Surgery, School of Life Dentistry at Tokyo, The Nippon Dental University, Tokyo, Japan

[3]Pikos Institute, Tampa, Florida, USA

[4]Department of Periodontology, Kagoshima University Graduate School of Medical and Dental Sciences, Kagoshima, Japan

[5]Department of Oral Implantology, University of Wuhan, Wuhan, China

Correspondence
Richard J. Miron, Department of Periodontology, University of Bern, 9280 Coral Isles Circle, Palm Beach Gardens, Florida, 33412, USA.
Email: rick@themironlab.com

Abstract

Bone grafts are typically categorized into four categories: autografts, allografts, xenografts, and synthetic alloplasts. While it was originally thought that all bone grafts should be slowly resorbed and replaced with native bone over time, accumulating evidence has in fact suggested that the use of nonresorbable xenografts is favored for certain clinical indications. Thus, many clinicians take advantage of the nonresorbable properties/features of xenografts for various clinical indications, such as contour augmentation, sinus grafting, and guided bone regeneration, which are often combined with allografts (e.g., human freeze-dried bone allografts [FDBAs] and human demineralized freeze-dried bone allografts [DFDBAs]). Thus, many clinicians have advocated different 50/50 or 70/30 ratios of allograft/xenograft combination approaches for various grafting procedures. Interestingly, many clinicians believe that one of the main reasons for the nonresorbability or low substitution rates of xenografts has to do with their foreign animal origin. Recent research has indicated that the sintering technique and heating conducted during their processing changes the dissolution rate of hydroxyapatite, leading to a state in which osteoclasts are no longer able to resorb (dissolve) the sintered bone. While many clinicians often combine nonresorbable xenografts with the bone-inducing properties of allografts for a variety of bone augmentation procedures, clinicians are forced to use two separate products owing to their origins (the FDA/CE does not allow the mixture of allografts with xenografts within the same dish/bottle). This has led to significant progress in understanding the dissolution rates of xenografts at various sintering temperature changes, which has since led to the breakthrough development of nonresorbable bone allografts sintered at similar temperatures to nonresorbable xenografts. The advantage of the nonresorbable bone

This is an open access article under the terms of the Creative Commons Attribution License, which permits use, distribution and reproduction in any medium, provided the original work is properly cited.
© 2024 The Authors. *Periodontology 2000* published by John Wiley & Sons Ltd.

allograft is that they can now be combined with standard allografts to create a single mixture combining the advantages of both allografts and xenografts while allowing the purchase and use of a single product. This review article presents the concept with evidence derived from a 52-week monkey study that demonstrated little to no resorption along with in vitro data supporting this novel technology as a "next-generation" biomaterial with optimized bone grafting material properties.

KEYWORDS
allograft, anorganic bovine bone mineral, Bio-Oss, deproteinized bovine bone mineral

1 | INTRODUCTION

To develop or maintain optimal dimensional stability in alveolar bone to support teeth and implants, sufficient bone volume in the vertical and horizontal dimensions is mandatory.[1] For these reasons, bone grafting materials have played a pivotal role in modern dentistry. The concept of utilizing bone grafting materials has a history of more than 30 years. Procedures such as 'guided tissue/bone regeneration' (GTR/GBR) were introduced to the field of periodontology and implant dentistry to promote new alveolar bone formation in deficient tissues.[2–5]

Today, more than 100 bone grafting materials exist on the market. These include autografts (derived from the same patient), allografts (derived from a human cadaver), xenografts (derived from other animal species and plants), and synthetically fabricated alloplasts.[6] Each of these classes of bone grafts offers various advantages and disadvantages based on their respective handling properties, biocompatibility, surface geometry and chemistry, mechanical properties, and degradation properties. While autogenous bone is considered the gold standard combining the features of osteoconduction, osteoinduction and osteogenesis, as highlighted in the previous article titled "Optimized bone grafting",[7] alternative bone grafting materials available in higher supply with less patient morbidity have always been a desired end goal for clinicians.

Bone allografts are an excellent replacement option with good osteoconductive properties and certain types are known to be osteoinductive due to their release of bone morphogenetic proteins (BMPs) in demineralized freeze-dried bone allografts (DFDBAs).[8] Xenografts on the other hand are also a highly utilized bone grafting material, especially in countries where the use of allografts is not permitted. Xenografts were first developed to act as a standard replacement material similar to allografts, it has since been revealed that unlike allografts, xenografts typically do not resorb over time, and in particular, the intensively studied deproteinized bovine bone mineral (DBBM, Bio-Oss®, Geistlich, Switzerland) has been characterized as a nonresorbable material in many studies due to its histological stability over time. This article first highlights the use of xenografts in regenerative dentistry with special attention to DBBM grafting particles as a nonresorbable material. Thereafter, an improved understanding of the dissolution rates of DBBM is addressed, including the graft material changes made as sintering takes place at higher temperatures. Thereafter, an approach to the sintering of bone allografts similar to that of xenografts, at temperatures ranging from 300 to 1300°C for 1–4 h, is presented. In vitro data investigating their regenerative properties along with 16- and 52-week data in monkeys confirm their nonresorptive properties when sintered at high temperatures. This work provides the groundwork for the fabrication of nonresorbable bone allografts (NRBAs) and highlights the impact of combining them with standard allografts in various ratios to obtain a single next-generation biomaterial for bone grafting.

2 | BIOLOGICAL BACKGROUND: USE OF NONRESORBABLE MATERIALS

While it was initially relatively unknown to what extent bone resorption would occur following bone augmentation procedures with xenografts, the most prominent advantage of these biomaterials remains that bone augmented with xenografts seemed to maintain their structure even years following their surgical implantation. Unlike allografts, which are prone to dimensional resorption over time, xenografts maintain their volume owing to their nonresorbable properties. Accordingly, a variety of procedures in dentistry have since been adapted to take advantage of these low-substitution rate materials.

The most widely used xenograft in the world is DBBM (Bio-Oss®, Geistlich, Switzerland). Today, DBBM is perhaps the most widely researched bone grafting material in the dental field, with widespread use throughout the world. It is also understood that the main advantage of DBBM is that it maintains volume, and the graft is deemed low- or nonresorbing (Figure 1).[9] Accordingly, DBBM particles have been utilized in a number of clinical applications, including contour augmentation in implant dentistry (especially in the esthetic zone), filling narrow gaps in immediate implant placement, sinus augmentation procedures, vertical augmentation procedures, and major bone reconstructive surgery following cancer. As reviewed previously, xenografts typically are not able to elicit much osteoinduction to the graft and have limited or no ability to affect cell recruitment owing to their lack of growth factor incorporation (deproteinized/anorganic bovine bone mineral), yet possess the ability to remain within defect sites even years after their implantation.[9]

16000757, 0, Downloaded from https://onlinelibrary.wiley.com/doi/10.1111/prd.12551 by Universitat Bern, Wiley Online Library on [08/02/2024]. See the Terms and Conditions (https://onlinelibrary.wiley.com/terms-and-conditions) on Wiley Online Library for rules of use; OA articles are governed by the applicable Creative Commons License

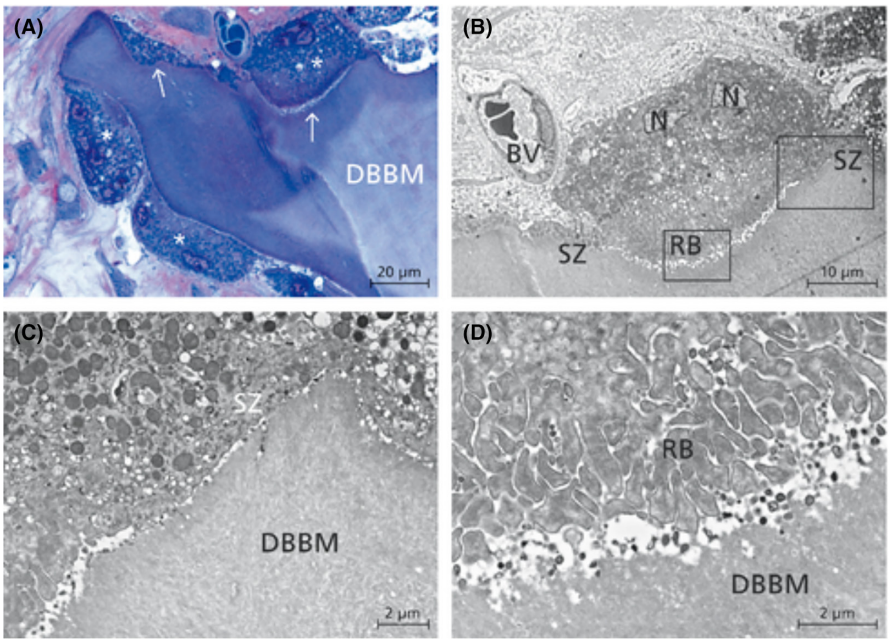

FIGURE 1 (A) Multinucleated giant cells (MNGCs) (*) situated on a deproteinized bovine bone mineral (DBBM) surface of a particle placed in the soft tissue outside the bone defect. Pronounced resorption lacunae are seen (arrows). (B) TEM magnification of the upper right region in (A). A multinucleated giant cell with two nuclei (N) in a resorption lacuna on DBBM. A blood vessel (BV) is seen directly next to the MNGC, which is common during bone remodeling. The MNGC demonstrates a sealing zone (SZ) and ruffled border (RB). (C) Higher magnification of the sealing zone (SZ). (D) Higher magnification of the ruffled border (RB). Reprinted with permission from Jensen et al.[9]

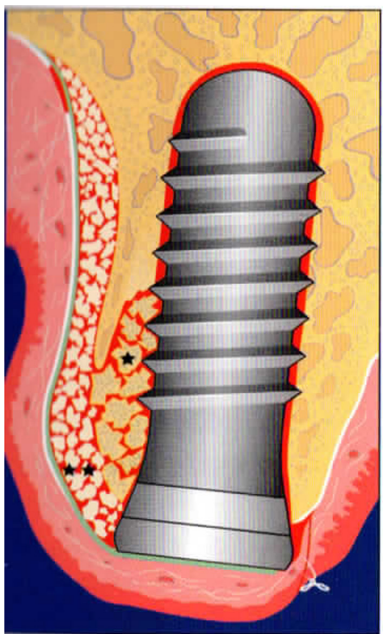

FIGURE 2 Illustration demonstrating early implant placement in the aesthetic zone. Implants are placed slightly palatally following 8 weeks of healing. In this dual-layer bone grafting procedure, autogenous bone chips (*) cover the exposed implant surface and are augmented with a second layer of low-substitution filler DBBM (**). The augmentation material is covered with a collagen membrane as a temporary barrier. The biomaterials are protected by tension-free primary wound closure. Reprinted with permission from Buser "20 years of Guided bone regeneration in implant dentistry".

2.1 | Clinical indications for using xenografts

The previous article titled "Optimized Bone Grafting"[7] highlighted the various roles and indications for the use of xenografts in implantology. One of the main applications has been its use as a preferred graft for contour grafting (also often referred to as veneer grafting). Figure 2 illustrates such a layering technique, where autogenous bone is utilized adjacent to the implant surface, and sintered xenografts are commonly used as an outer layer because their low substitution rate/nonresorbability allow better maintenance over time. This technique combines the advantages of the highly osteogenic/osteoinductive autograft on the implant surface to speed bone-to-implant contact with nonresorbable DBBM particles on the outer surface to contour the bone and act as a "shield." From a surgical standpoint, in the esthetic zone, contour augmentation procedures are typically performed after an 8-week healing period following tooth extraction to allow sufficient soft tissue regrowth and bone remodeling (and buccal plate resorption) to take place.

Similarly, xenografts have been heavily utilized and studied during sinus grafting procedures. Many clinicians have further advocated a mixture of DBBM and freeze-dried bone allograft (FDBA) mixed in a 50:50 ratio to take advantage of both the nonresorbability of xenografts and the better bone-inducing properties of allografts.[10,11] Similarly, vertical bone augmentations often relapse following bone growth. Therefore, nonresorbable xenografts have been added to autografts and/or allografts to maintain bone long term.[10,11]

3 | UNDERSTANDING SINTERING AND TEMPERATURE CHANGES OF ALLOGRAFTS AND XENOGRAFTS

In recent years, there has been a notable increase in scholarly investigations pertaining to burnt bone analysis. This surge has contributed to a more nuanced comprehension of the intricate transformations within the bone matrix during burning at varying temperature levels. Moreover, these transformations have yielded valuable insights into the interpretive potential of skeletal remains. Consequently, numerous scholarly articles have been published offering comprehensive

16000757, 0, Downloaded from https://onlinelibrary.wiley.com/doi/10.1111/prd.12551 by Universitat Bern, Wiley Online Library on [08/02/2024]. See the Terms and Conditions (https://onlinelibrary.wiley.com/terms-and-conditions) on Wiley Online Library for rules of use; OA articles are governed by the applicable Creative Commons License

overviews of the latest advancements in the field of burnt bone analysis.[12–16]

Essentially, heated bone goes through a series of four changes.[15,16] First, it undergoes dehydration, where the hydroxyl bonds break, and water loosely bound to the bone structure is lost. Second, decomposition occurs, during which pyrolysis eliminates the organic constituents of the bone. The third stage is inversion, where the bone loses its carbonate content. The fourth and final stage is fusion, where the crystal matrix of the bone melts and merges. The different phases of micro- and nano-structural transformations result in noticeable changes in various aspects of bones, including their color, shape, internal structure, mechanical properties, and crystal arrangement. When bones are subjected to fire, they go through several well-defined stages, collectively referred to as 'burnt bone'. Specifically, "charred bone" pertains to bone that has come into direct contact with a heat source, leading to a blackened appearance caused by the carbonization of both skeletal material and soft tissue. Bone that has undergone a process known as "calcination" or "incineration" has been subjected to high temperatures, resulting in the complete removal of all organic components and moisture. This transforms the bone into a white, distorted, "fractured state".[17]

Differential scanning calorimetry (DSC) and thermogravimetric analysis (TGA) are methods used to analyze the thermal behavior of materials as they are heated. These techniques provide valuable information regarding the properties of materials and their phase transitions under various temperature conditions.[18–23] During these investigations, researchers have used a combined TGA-DSC approach to examine how varying temperatures and heating rates affect the decomposition of hard tissue in the skeletal structure.

The study's findings revealed important insights. First, when subjected to rapid heating, the bone matrix showed a delay in the onset of phase changes, requiring higher temperatures for these changes to begin. Second, the progression of matrix changes within a specific phase was significantly influenced by the heating rate. Slower heating rates or prolonged exposure times promoted the advancement of decomposition within a given phase. However, it was observed that the transition to a different material phase only occurred after reaching a critical "activation temperature."[24]

The structure of the bone's extracellular matrix is made up of three primary components: a mineral phase, making up approximately 65% of its weight; an organic phase, constituting approximately 25% of its weight; and water, comprising the remaining 10% of its weight.[25] The mineral phase comprises a hydroxyapatite variant known as dahllite, which exhibits poor crystallinity and nonstoichiometry. This form of hydroxyapatite ($Ca_{10}(PO_4)_6(OH)_2$) contains many elemental replacements, including but not limited to magnesium and other ions. Among these substitutions, carbonate is the most prevalent, accounting for approximately 3–8% by weight.[18]

The primary constituent of the organic matrix is type I collagen, whereas other constituents consist of noncollagenous organic proteins, particularly phosphoproteins. These phosphoproteins may contribute to the control of crystal dimensions, alignment, and structure within the mineral matrix.[26,27]

The existing body of research confirms the weight loss patterns seen in heated bone, which may be categorized into three distinct phases (Figure 3). The first stage occurs at temperatures below 200°C, followed by a second stage between 200 and 600°C, and finally, a third stage between 700 and 900°C. Weight loss has been shown to be insignificant at temperatures over 900°C.[18–22] The first stage of weight loss is associated with the release of water attached to the bone matrix, referred to as the "dehydration" phase. The subsequent stage, known as the "decomposition" phase, is ascribed to the breakdown of the organic components of the bone, namely, collagen, by combustion. The last stage of weight loss mostly occurs as a result of the liberation of carbon dioxide (CO_2) generated during carbonate breakdown. The presence of hydroxide ions is seen in conjunction with the recrystallization of the mineral apatite during the "inversion" phase. The concluding stage of bone transformation, which takes place at temperatures over 900°C, is often referred to as the "fusion" phase. In this phase, a substantial reduction in weight is not seen. Instead, the primary features of this phase are the melting of the crystallites and the process of sintering, together with the emergence of a new mineral phase known as β-tricalcium phosphate (β-TCP).[13,23]

The second stage of weight loss, known for its heightened intensity, may be linked to burning organic components, leading to the exothermic process of hydroxyapatite recrystallization. The dissolution of carbonate at approximately 450°C is accompanied by a short endothermic phase, followed by a pronounced exothermic phase when the collagen in the bone undergoes combustion, reaching its peak at approximately 500°C. Concurrently, the recrystallization of minerals takes place. The exothermic nature of the process persists until reaching temperatures of 750–800°C, beyond which the minerals undergo sintering and melting, resulting in a somewhat endothermic phase.

4 | UNDERSTANDING DISSOLUTION RATES OF HYDROXYAPATITE FOLLOWING SINTERING

Despite the extensive body of research dedicated to examining the dissolution rates of different ceramics, the understanding of the biological, chemical, and physical factors behind the process of bioresorption in bone grafts remains limited. Notably, two great studies investigating this topic have been published previously by Marc Bohner's group in Switzerland.[28,29] The three main parameters involved in bioresorption have previously been reported as (1) solubility, (2) kinetics, and (3) in vivo conversion.[29] The aforementioned calcium phosphates (CaPs) are of special importance in the context of in vivo applications due to their presence in living organisms, which distinguishes them from conventionally implanted CaPs such as β-tricalcium phosphate (β-TCP; Ca3(PO4)2) and sintered hydroxyapatite (sintered HA; Table 1).[29–31] The medical field mostly employs high-temperature calcium phosphates (CaPs) with typical characteristics, such as β-TCP, hydroxyapatite (HA), and bicalcium phosphate (BCP) composites consisting of β-TCP and HA.[28]

16000757, 0, Downloaded from https://onlinelibrary.wiley.com/doi/10.1111/prd.12551 by Universitat Bern, Wiley Online Library on [08/02/2024]. See the Terms and Conditions (https://onlinelibrary.wiley.com/terms-and-conditions) on Wiley Online Library for rules of use; OA articles are governed by the applicable Creative Commons License

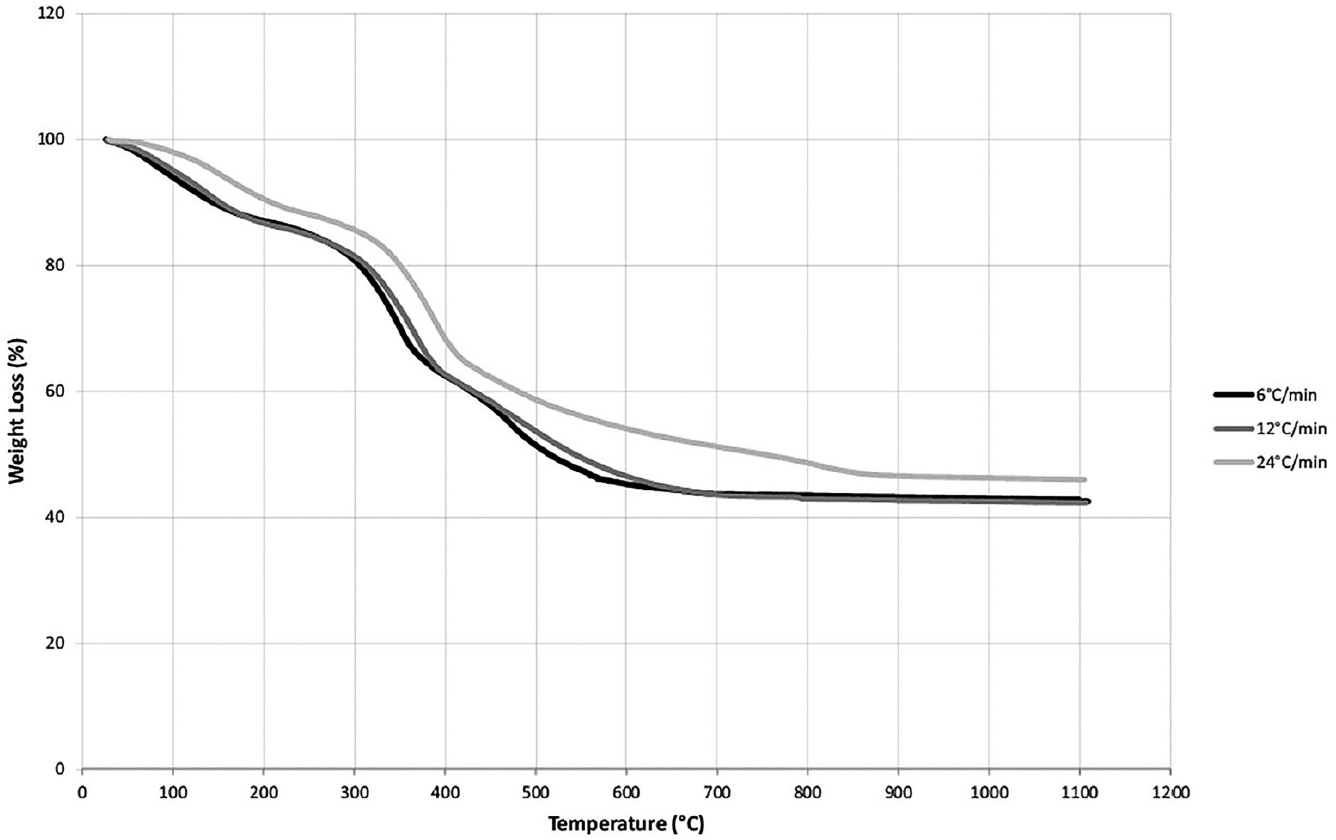

FIGURE 3 Average thermogravimetric analysis (TGA) curves of bones subjected to differing heating regimes. Reprinted with permission.[24]

TABLE 1 Main calcium phosphate compounds (CPC): the first six compounds precipitate at room temperature in aqueous systems; the last six compounds are obtained by thermal decomposition or thermal synthesis.

Name	Formula	Ca/P (molar)	Mineral	Symbol	In vivo behavior
Monocalcium phosphate monohydrate	$Ca(H_2PO_4)_2 H_2O$	0.50	–	MCPM	Biosoluble
Dicalcium phosphate	$CaHPO_4$	1.00	Monetite	DCP	Biosoluble
Dicalcium phosphate dihydrate	$CaHPO_4 2H_2O$	1.00	Brushite	DCPD	Biosoluble
Octacalcium phosphate	$Ca_8H_2(PO_4)_6 5H_2O$	1.33	–	OCP	Bioresorbable
Precipitated hydroxyapatite[a]	$Ca_{10-x}(HPO_4)_x(PO_4)_{6-x}(OH)_{2-x}$	1.33–1.67	–	PHA	Bioresorbable
Amorphous calcium phosphate	$Ca_3(PO_4)_2nH_2O$ where $n=3$–4.5; 15–20% H_2O	1.50	–	ACP	Biosoluble
Monocalcium phosphate	$Ca(H_2PO_4)_2$	0.50	–	MCP	Biosoluble
α-Tricalcium phosphate	α-$Ca_3(PO_4)_2$	1.50	–	α-TCP	Biosoluble
β-Tricalcium phosphate	β-$Ca_3(PO_4)_2$	1.50	–	β-TCP	Bioresorbable
Sintered hydroxyapatite	$Ca_{10}(PO_4)_6(OH)_2$	1.67	Hydroxyapatite	SHA	Bioresorbable
Oxyapatite	$Ca_{10}(PO_4)_6O$	1.67	–	OXA	Bioresorbable
Tetracalcium phosphate	$Ca_4(PO_4)_2O$	2.00	Hilgenstockite	TetCP	Biosoluble

[a]Tricalcium phosphate (TCP) $Ca_9(HPO_4)(PO_4)_5(OH)$ is a subcategory of PHA.

4.1 | β-tricalcium phosphate (β-TCP; β-$Ca_3(PO_4)_2$)

β-TCP may be synthesized using a thermal process at temperatures above 650°C.[32] Other potential approaches may also be considered. One option involves creating a combination consisting of equal amounts of dicalcium phosphate dihydrate (DCPD) and precipitated HA (PHA) with a calcium-to-phosphorus (Ca:P) ratio of 1.67, followed by calcination. Another approach involves directly subjecting PHA with a Ca:P ratio of 1.50 to calcination. It is important to differentiate β-TCP from TCP due to their almost identical

16000757, 0, Downloaded from https://onlinelibrary.wiley.com/doi/10.1111/prd.12551 by Universitat Bern, Wiley Online Library on [08/02/2024]. See the Terms and Conditions (https://onlinelibrary.wiley.com/terms-and-conditions) on Wiley Online Library for rules of use; OA articles are governed by the applicable Creative Commons License

chemical content but distinct crystallographic structures. TCP has an apatite-like structure and exhibits a Ca:P molar ratio of 1.50, which is consistent with that of phosphate-based hydroxyapatite (PHA). β-TCP in the form of either granules or blocks has been widely used as a bone replacement. β-TCP exhibits degradability via osteoclastic activity.[33]

4.2 | α-tricalcium phosphate (α-TCP; α-$Ca_3(PO_4)_2$)

α-TCP and β-TCP possess identical chemical compositions but distinct crystallographic structures. The dissimilarity between α-TCP and β-TCP results in higher solubility of α-TCP than β-TCP. The production of α-TCP typically involves subjecting β-TCP to temperatures over 1125°C, followed by rapid cooling to impede the reverse transition.[34] α-TCP may be easily converted into PHA with a molar ratio of 1.50 of calcium to phosphorus in aqueous solution. This characteristic is employed in the production of apatite CPC. α-TCP has emerged as the predominant constituent in the majority of apatite CPCs. The biocompatibility of α-TCP is superior to that of β-TCP, and it also exhibits higher biodegradability.

4.3 | Biphasic calcium phosphate (BCP; β-TCP-HA composite)

BCP is made up of β-TCP-HA. It is produced by calcining PHA at temperatures over 700°C with a molar ratio Ca:P < 1.67.[35,36] The degradability of BCP is higher than that of HA. The rate of degradation has a positive correlation with the concentration of β-TCP. The majority of commercial products consist of 40% β-TCP and 60% HA.

4.4 | Hydroxyapatite (HA; $Ca_5(PO_4)_3OH$)

The term "HA" is hereby designated as the high-temperature variant of a stoichiometric PHA, with a minimum temperature requirement of 700°C. HA exhibits a high degree of crystallinity and is regarded as the most stable CaP compound when dissolved in an aqueous medium. Furthermore, HA is widely acknowledged as the most biocompatible CaP material. At temperatures ~900°C, there is a possibility of partial breakdown occurring in HA, ultimately leading to the formation of oxyapatite (OXA). This chemical reaction occurs only in the absence of water vapor.[37] HA, partly dehydrated HA or OXA undergoes thermal decomposition at temperatures over 1300°C, resulting in the formation of tetracalcium phosphate (TetCP) and α-TCP. The latter reaction exhibits an increased rate in the absence of water vapor.[38] The majority of bone replacements on the market today consist of HA. Because these items' degradation times are measured in decades rather than years, they should be classified as nondegradable.[28]

4.5 | In vivo behavior of ceramic bone

In vivo investigations conducted by previous research groups using several ceramics have shown significant disparities in their in vivo characteristics.[39,40] In one study, calcium sulfate dihydrate (CSD; CaSO4·2H2O; Table 2) underwent dissolution within a few weeks after its introduction into the implantation defect,[41] whereas sintered HA has been projected to last several centuries.[42] The observed distinctions may be attributed in part to the geometric characteristics[43] and in part to the chemical properties of the entities in question.[44,45] Several investigations have been conducted to ascertain the impact of geometry on bone ingrowth and the pace at which bone substitutes are removed using either experimental[46–51] or theoretical methodologies. Much research has also been done on how the nature of bioresorbable ceramics affects how they act in the body, with either an in vitro,[52–56] an in vivo,[43,57–63] or a theoretical approach.[64–67]

When considering the in vivo behavior of ceramic bone replacements, it is crucial to take into account three key features. The first is the molecule's solubility inside the human body. If the drug exhibits solubility under certain physiological circumstances, it may undergo dissolution, thereby leading to its elimination. The second is the rate at which the specific ceramic material is extracted from the body, specifically referring to its dissolution kinetics. Empirical investigations demonstrate that the solubility of a substance does not always guarantee its dissolution.[92]

The third feature is the propensity for conversion into another component via a dissolution-precipitation process. Among calcium phosphates, apatites exhibit the highest degree of stability under physiological settings. Hence, nonapatitic CaP compounds, when introduced into bone, tend to transform into apatite. The three aforementioned elements, namely, solubility, dissolution, and conversion, exhibit a strong interrelationship while maintaining their own autonomy. One example of a bioresorbable ceramic that exhibits solubility inside the human body is α-TCP. However, its in vivo conversion into apatite may require many years.

4.6 | Solubility of bone grafts

According to Driessens et al.,[66] the solubility-controlling phase in live bone is known as OCP (octacalcium phosphate), and its presence plays a regulatory role in maintaining the concentrations of CaP throughout the body via physicochemical equilibrium. Consequently, calcium phosphates (CaPs) that exhibit higher solubility than octacalcium phosphate (OCP) under physiological conditions, including dicalcium phosphate (DCP), dicalcium phosphate dihydrate (DCPD), alpha-tricalcium phosphate (α-TCP), tetracalcium phosphate (TetCP; $Ca_4(PO_4)_2O$), monocalcium phosphate (MCP; $Ca(H_2PO_4)_2$), and monocalcium phosphate monohydrate (MCPM; $Ca(H_2PO_4)_2{\cdot}H_2O$), are anticipated to dissolve spontaneously. Conversely, CaPs with lower solubility than OCP under physiological conditions, such as

16000757, 0, Downloaded from https://onlinelibrary.wiley.com/doi/10.1111/prd.12551 by Universitat Bern, Wiley Online Library on [08/02/2024]. See the Terms and Conditions (https://onlinelibrary.wiley.com/terms-and-conditions) on Wiley Online Library for rules of use; OA articles are governed by the applicable Creative Commons License

TABLE 2 Non-exhaustive list of doped CaP ceramics and non-CaP ceramics proposed for in vivo use.

Name	Formula	Ca/P (molar)	Mineral	Symbol	In vivo behavior
Carbonated apatite	$Ca_{8.8}(HPO_4)_{0.7}(PO_4)_{4.5}(CO_3)_{0.7}(OH)_{1.3}$	1.96	Dahlite	CA	Bioresorbable
Calcium carbonate[59,60,68]	$CaCO_3$	–	Calcite	–	Bioresorbable
Calcium carbonate[68,69]	$CaCO_3$	–	Aragonite	–	Bioresorbable
Calcium carbonate	$CaCO_3$	–	Vaterite	–	Biosoluble
Calcium magnesium silicate[70,71]	$Ca7MgSi_4O_{16}$	–	Bredigite	–	?
Calcium metaphosphate[72–75]	$Ca\ (PO_3)_2$	0.50	–	–	Biosoluble to bioresorbable[a]
Calcium potassium phosphate[76]	$CaKPO_4$	1.00	–	–	Biosoluble
β-Calcium pyrophosphate[77–80]	$\beta\text{-}Ca_2P_2O_7$	1.00	–	CPP	Bioresorbable
Calcium silicate[81]	$CaSiO_3$	–	Wollastonite	–	Biosoluble
Calcium silicate[82]	$CaSiO_3$	–	Pseudowollastonite	–	Biosoluble
Calcium silicate -phosphate composite[83,84]	$CaSiO_3$ - $Ca_3(PO_4)_2$	–	–	–	Bioresorbable
Calcium sodium Phosphate[85,86]	$CaNaPO_4$	1.00	Rhenanite	–	Biosoluble
Calcium sodium potassium phosphate[52]	$Ca_2\ NaK(PO_4)_2$	1.00	–	–	Biosoluble
Calcium sulfate hemihydrate[87]	$CaSO_4{\cdot}½H_2O$	–	Plaster of Paris	CSH	Biosoluble
Calcium sulfate dihydrate[88]	$CaSO_4{\cdot}2H_2O$	–	Gypsum	CSD	Biosoluble
Silicon-substituted tricalcium phosphate[89,90]	$Ca_{3.08}(P_{0.92}Si_{0.08}O_4)_2$ or $Ca_3(P_{0.9}Si_{0.1}O_{3.95})_2$	>3	–	–	Bioresorbable
Silicon-substituted hydroxyapatite[91]	$Ca_{10}(PO_4)_{6\text{-}x}{\cdot}(SiO_4)_{\cdot x}(OH)_{2\text{-}x}$	1.73 ($x=0.19$)	–	–	Bioresorbable

[a]Depends on the degree of crystallinity.

16000757, 0, Downloaded from https://onlinelibrary.wiley.com/doi/10.1111/prd.12551 by Universitat Bern, Wiley Online Library on [08/02/2024]. See the Terms and Conditions (https://onlinelibrary.wiley.com/terms-and-conditions) on Wiley Online Library for rules of use; OA articles are governed by the applicable Creative Commons License

β-TCP and sintered-HA, can only be dissolved through active involvement of cells. Certain types of cells, such as osteoclasts and macrophages, have the ability to decrease the pH[93] in their immediate surroundings. This reduction in pH can lead to the dissolution and subsequent resorption of certain ceramics, such as CaPs or calcium carbonates, which are known to be more soluble at low pH (Figure 4).[94] For a more comprehensive understanding of the cellular processes involved in bioresorption, please refer to the research paper by Koerten and van der Meulen.[58] The solubility of the ceramic material plays a crucial role in determining its resorption process. Therefore, it is essential to highlight the distinction between ceramics with higher and solubility than OCP. The word 'biosoluble' is used to refer to ceramics with greater solubility than OCP, whereas the phrase 'bioresorbable' is used to describe ceramics with lower solubility than OCP.

Within the existing body of research, there exists a substantial amount of empirical evidence of the superior bioresorbability of β-TCP in comparison to sintered HA.[95,96] Additionally, there is evidence that DCPD has a higher in vivo clearance rate than β-TCP.[97] Other findings demonstrate that OCP has a higher in vivo clearance rate than HA and β-TCP30.[98]

Until now, the consideration of two significant variables impacting solubility has been overlooked: the stoichiometry and the dimensions of the crystals. The impact of these two factors on solubility is substantial. Regarding stoichiometry, Liu et al.[99] documented a significant change in the solubility of polyhydroxyalkanoates (PHAs) when the molar ratio of calcium to phosphorus (Ca/P) was decreased from 1.67 to 1.50. Regarding crystal size, it is often seen that precipitated calcium phosphates, such as PHA, exhibit micro- or nanoscale dimensions. When crystals are reduced to nanometric dimensions,

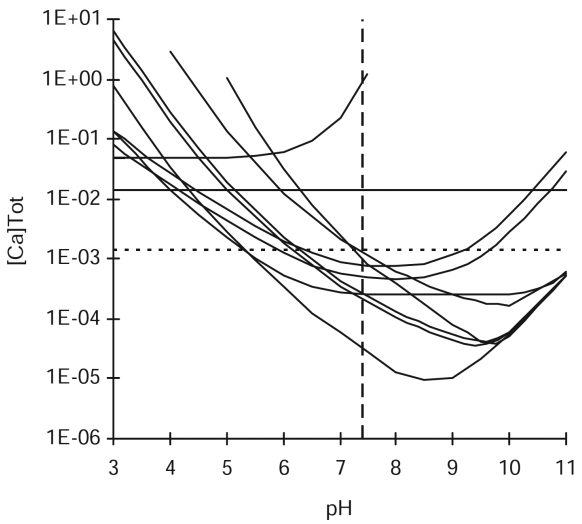

FIGURE 4 Solubility isotherms of calcium-based bone substitutes at 25°C in water. At pH 7.4, the solubility curves are from top to bottom: MCPM, CSD, α-TCP, TetCP, DCPD, DCP, OCP, CPP (flat curve), CDHA (parallel to β-TCP), β-TCP, and sintered HA. The dashed line represents the concentration of calcium ions in human serum/blood. Reprinted with permission from Turitto and Flack.[103]

the contribution of the crystal surface energy becomes significant in relation to the overall crystal energy. Consequently, the crystal exhibits lower thermodynamic stability.

4.7 | In vivo transformation of bone grafts

Biosoluble CaPs, which are inherently soluble inside living organisms (in vivo),[66] may be effectively eliminated from the body via dissolution and subsequent ionic transport. Nevertheless, the ions that are liberated via the dissolution of these compounds have the potential to interact with bodily fluids, resulting in the creation of novel molecules with reduced solubility.[100]

At physiological pH, hydroxyapatite is the most stable component of CaP (Figure 4). Hence, it can be concluded that all calcium phosphates, with the exception of hydroxyapatite, exhibit thermodynamic instability under these circumstances. Consequently, they are expected to undergo conversion to hydroxyapatite or an apatitic compound. This is mostly due to the ability of hydroxyapatite to readily integrate foreign ions, such as carbonates, sulfates, magnesium, sodium, and others.

4.8 | Modeling resorption

The understanding of the in vivo performance of CaP materials may be significantly enhanced by the use of solubility data. Nevertheless, can the in vivo behavior be predicted using solubility data? Can the rate of DCP removal from the implantation site be predicted relative to β-TCP, assuming constant geometry? The conventional methodology used for predicting the in vivo performance of CaP bone replacements involves conducting dissolution studies and basing predictions on the obtained data.

While most cells have a pH of approximately 7.4, those responsible for removing calcium phosphates (osteoclasts and macrophages) have pH values lower than 7.4. For example, according to the findings of Silver et al.,[93] the pH values observed for osteoclasts were approximately 3.0 or lower, whereas macrophages exhibited pH values ranging from 3.6 to 3.7. Hence, it is logical to replicate the in vivo dynamics by assessing the dissolution kinetics throughout a pH spectrum spanning from 3 to 7.4. Chow et al.[53] used a pH value of 3.0 and noted that the dissolution rate of DCPD was three times higher than that of sintered HA. This disparity seems rather insignificant when considering the context of in vivo conditions.[39,101]

Bioresorbable CaP is eliminated through a dynamic mechanism characterized by two main steps. First, there is a reduction in the pH level the normal physiological range to an acidic pH, typically approximately pH 3–4.[93] This acidic environment causes CaP to become thermodynamically unstable and thus soluble. Second, the ceramic material dissolves, liberating neutral or basic ions. An instance of the release of Ca2+ and HPO4− ions occurs during the breakdown of DCP and DCPD. Hence, in the event that osteoclasts fail

16000757, 0, Downloaded from https://onlinelibrary.wiley.com/doi/10.1111/prd.12551 by Universitat Bern, Wiley Online Library on [08/02/2024]. See the Terms and Conditions (https://onlinelibrary.wiley.com/terms-and-conditions) on Wiley Online Library for rules of use; OA articles are governed by the applicable Creative Commons License

to generate sufficient acid to effectively reduce the pH to the levels required for the dissolution of CaP, CaP dissolution, and subsequent resorption do not occur. The successful modeling of the resorption process requires an understanding of the osteoclast acid generation rate, which is contingent upon the pH value. If the rate of acid generation is already known, it is possible to estimate the rate of resorption by measuring the dissolution rate of a CaP compound when exposed to an acidic environment that follows the acid production rate function.

5 | CONCEPTUALIZATION OF NONRESORBABLE BONE ALLOGRAFTS AND THEIR SINTERING

Once the dissolution rates and the related changes in hydroxyapatite were understood, a series of studies both in vitro and in vivo were undertaken by our research team to better understand the effects of ideal sintering temperatures and times on the ability of allografts to be deemed nonresorbable. Accordingly, standard allografts were sintered from 300 to 1300°C for 1–4 h to determine optimal sintering conditions. A representative scanning electron microscopy image is presented in Figure 5. Notably, the macroscopic images illustrate clear differences between the sintered and nonsintered bone (allograft). It could also be observed that the higher temperature sintered bone appeared smoother even on the macroscopic level. Sintered grafts, especially graphs sintered at high temperatures (greater than 1000 Celsius), showed greatly different surface textures from those of standard nonsintered FDBAs. Thereafter, the newly created grafts were tested both in vitro and in vivo.

6 | IN VITRO DATA ON THE BONE-INDUCING PROPERTIES OF ALLOGRAFTS, XENOGRAFTS AND NONRESORBABLE BONE ALLOGRAFTS

Prior to the accumulation of animal data, basic in vitro experiments were performed by our group to investigate the relationship of standard sintering techniques for FDBAs and DBBM and various sintering temperatures/times of bone allografts. As demonstrated in Figure 6A, the migration of cells was improved in all allograft groups when compared to control and DBBM samples. Typically, the proliferation of cells was also improved in the allograft groups compared to xenografts as well (Figure 6B). Polymerase chain reaction (PCR) experiments were increased in the standard allograft group at 3 days, but generally, all bone grafts were able to maintain collagen production irrespective of the graft utilized (Figure 6C). No significant difference was observed either with respect to alizarin red staining (Figure 6D). These combined findings seem to indicate that standard allografts have superior in vitro effects on bone formation, but both sintered xenografts and NRBAs exert equivalent effects on osteoblast activity, independent of sintering techniques. Thus, it was possible to further evaluate in vivo graft resorption/bone formation patterns at various temperatures over a 1-year period (52 weeks).

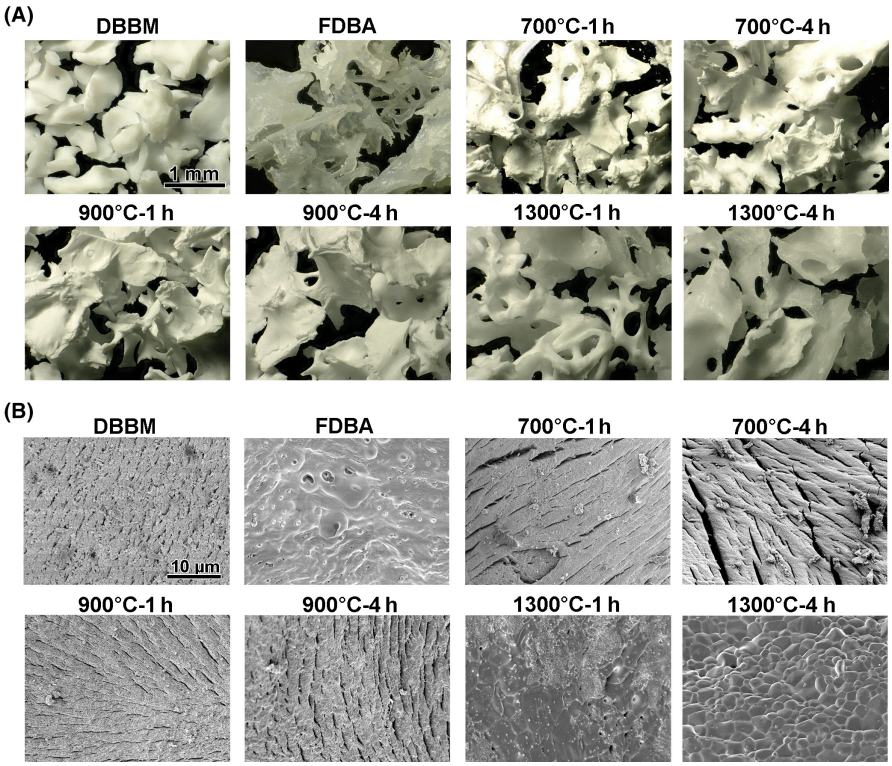

FIGURE 5 Scanning electron microscopy of bone grafting materials (both DBBM and allografts sintered at various temperatures/times) at both low and high magnification. Note the changes in surface topography once grafts are sintered at various temperatures.

16000757, 0, Downloaded from https://onlinelibrary.wiley.com/doi/10.1111/prd.12551 by Universitat Bern, Wiley Online Library on [08/02/2024]. See the Terms and Conditions (https://onlinelibrary.wiley.com/terms-and-conditions) on Wiley Online Library for rules of use; OA articles are governed by the applicable Creative Commons License

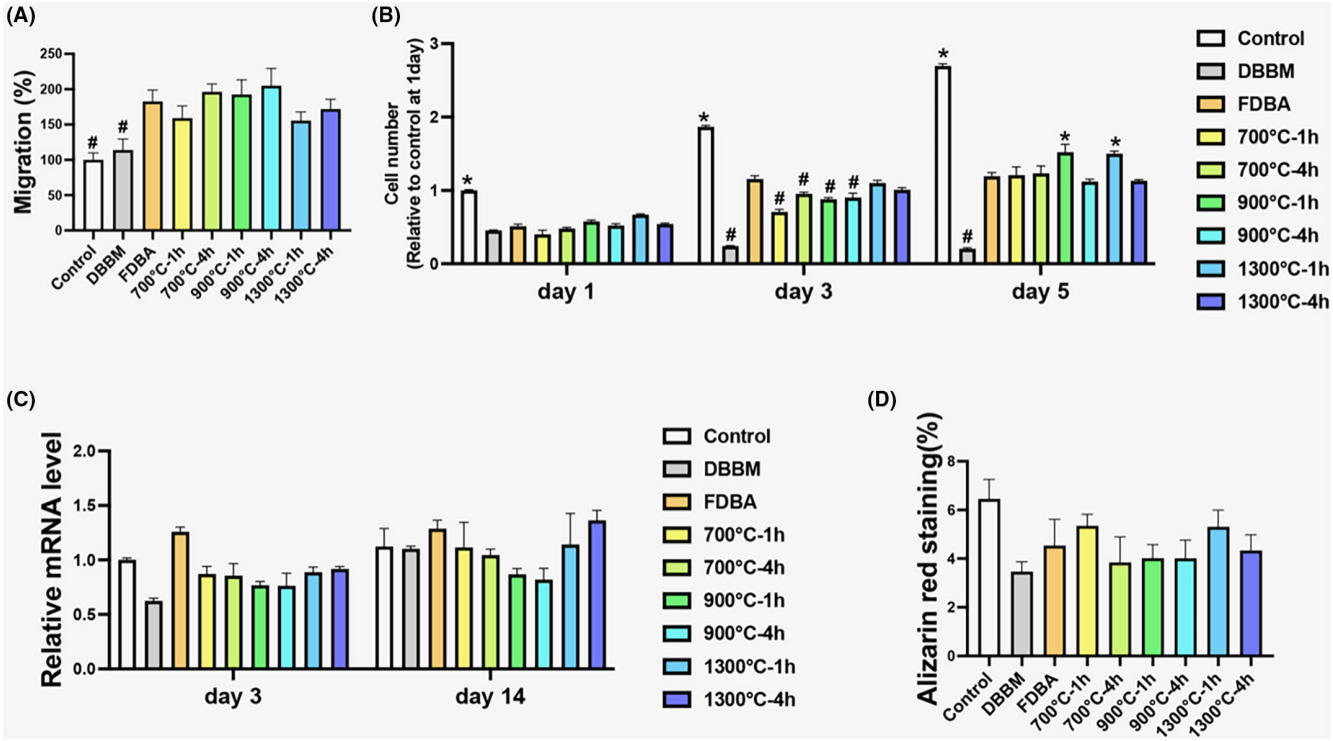

FIGURE 6 The effects of different bone substitutes (BSs) on osteoblast migration, proliferation, and differentiation. (A) Human primary osteoblast (HOB) migratory ability 24 h after stimulation with each BS treatment. The quantified data of migrated cell numbers were compared. All the FDBA BSs, including both nontreated and heat-treated BSs, promoted migratory potential when compared to control cell culture plastic and deproteinized bovine bone mineral (DBBM). (B) HOB proliferation potential on the different BS granules compared to control tissue culture plastic on Days 1, 3, and 5. The HOB viability and proliferation potential decreased compared with the control, whereas FDBA and the treated FDBA showed greater cell proliferation potential than DBBM over time. (C) Real-time PCR analysis of HOBs seeded on the BS granules was performed to assess the expression of the gene encoding *COL1* on Days 3 and 14 after osteoblast seeding. There were no significant differences in the mRNA levels of *COL1* between any BSs. (D) Alizarin red staining of HOBs for 14 days and the semiquantified results of HOBs cultured on the BS granules. All experiments were performed in triplicate with three independent experiments conducted per group. There was no significant difference in the mineralization potential of osteoblasts between any BS. * denotes significantly higher than nontreated FDBA ($p < 0.05$). # denotes significantly lower than nontreated FDBA ($p < 0.05$).

7 | IN VIVO EVALUATION IN MONKEYS OF BONE FORMATION/RESORPTION PATTERNS FOLLOWING IMPLANTATION OF ALLOGRAFTS, XENOGRAFTS, AND SINTERED ALLOGRAFTS IN EXTRACTION SOCKETS

Our research team then confirmed the in vivo properties of each of the sintered bone allografts in an animal model. Eight 7- to 8-year-old male monkeys (*Macaca fascicularis*) were selected for this study. Following intrasulcular incisions and elevation of mucoperiosteal flaps, both maxillary and mandibular lateral incisors, second premolars and second molars (i.e., 12 teeth/animal) were extracted. Extraction sockets were randomly filled with the following grafting materials (i.e., 6 teeth/group): (1) DBBM, (2) FDBA, (3) FDBA sintered at 700°C for 4 h, (4) FDBA sintered at 900°C for 1 h, (5) FDBA sintered at 900°C for 4 h, (6) FDBA sintered at 1300°C for 1 h, (7) FDBA sintered at 1300°C for 4 h, or (8) blood clot alone. The extraction sockets were covered by a resorbable collagen membrane (Bio-Gide®; Geistlich Pharma AG, Wolhusen, Switzerland). A periosteal releasing incision was made to allow tension-free coronal repositioning of the flap, followed by suturing (Gore-Tex CV-6 Suture, W. L. Gore & Associates Inc., Flagstaff, AZ, USA; Figure 7). All surgical treatments were well tolerated by the animals, and clinical healing was uneventful at all sites with limited signs of inflammation and limited gingival recession. No adverse reactions, including material exposure, increased tooth mobility, infection and suppuration, were observed throughout the entire experimental period. The animals (four animals for each observation period) were euthanized after 16 and 52 weeks. Microcomputed tomography (micro-CT) and histological analysis were used to evaluate the properties of the different biomaterials and bone formation in the extraction sites.

7.1 | Micro-CT findings

Two- and three-dimensional micro-CT images of the extraction sockets grafted with different biomaterials or blood clots acquired after 16 and 52 weeks are shown in Figures 8 and 9. Generally, bone remodeling on the buccal side was higher than that on the palatal/

16000757, 0, Downloaded from https://onlinelibrary.wiley.com/doi/10.1111/prd.12551 by Universitat Bern, Wiley Online Library on [08/02/2024]. See the Terms and Conditions (https://onlinelibrary.wiley.com/terms-and-conditions) on Wiley Online Library for rules of use; OA articles are governed by the applicable Creative Commons License

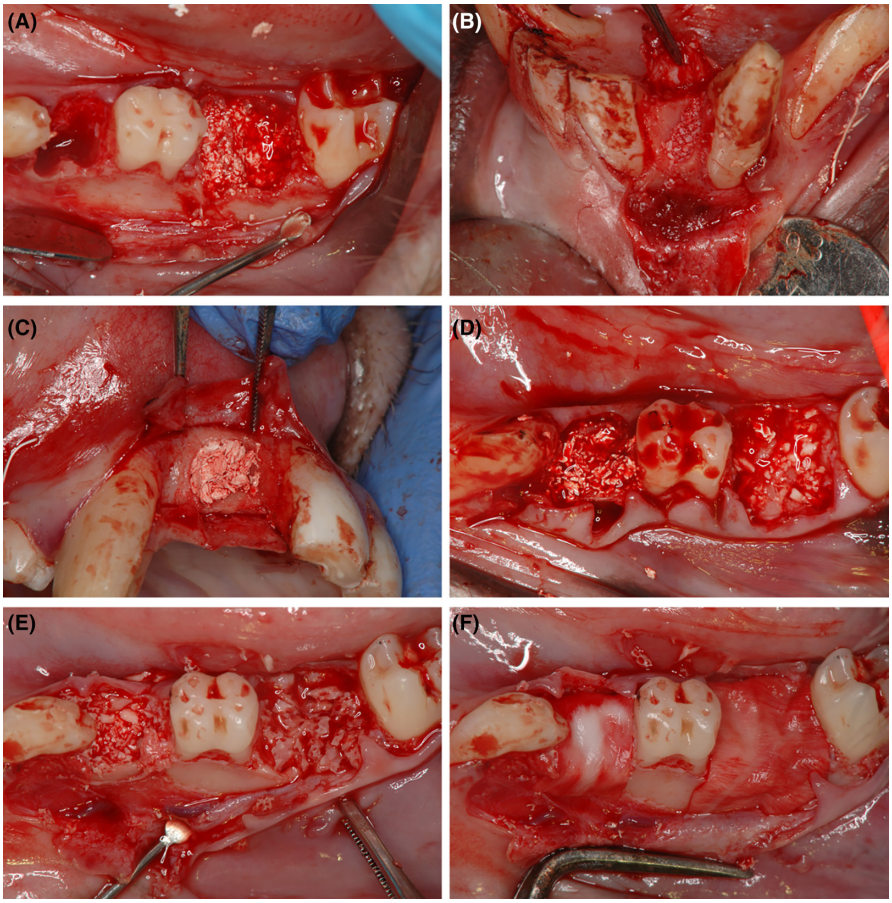

FIGURE 7 Overview of the surgical procedure: (A) The extraction sockets filled with blood clot (left) and FDBA sintered at 900°C for 1 h (right). (B) The extraction socket filled with DBBM. (C) The extraction socket was filled with FDBA sintered at 900°C for 4 h. (D) The extraction sockets filled with FDBA sintered at 700°C for 4 h (left) and 1300°C for 1 h (right). (E) The extraction sockets filled with FDBA sintered at 1300°C for 4 h (left) and FDBA (right). (F) All extraction sockets were covered by resorbable collagen membranes. All procedures were approved by the ethical committee of the Animal Research Center of Kagoshima University, Japan (approval no. D21027). This study conformed to the ARRIVE guidelines for preclinical animal studies.

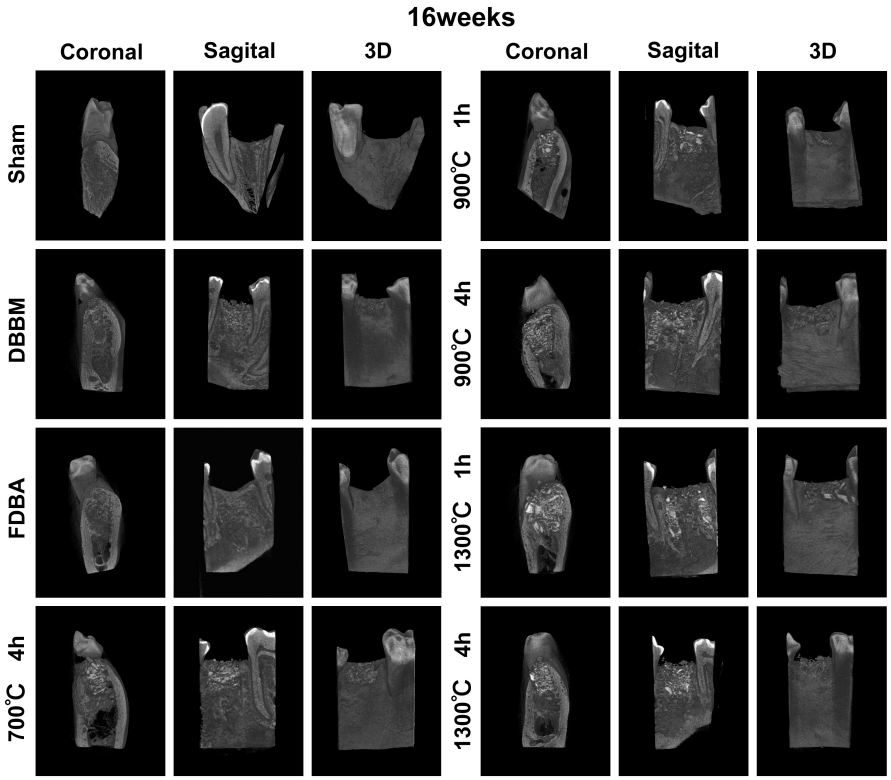

FIGURE 8 Micro-CT images of the extraction sockets in monkeys at 16 weeks.

lingual sides. Sixteen weeks after surgery, all control sites (sham group) exhibited low density and relatively low new bone formation with concave alveolar ridges. In the sites grafted with different biomaterials, varying degrees of residual bone graft particles and new bone formation within the extraction sockets were observed. For example, concave alveolar ridges were present in four of six sites

16000757, 0, Downloaded from https://onlinelibrary.wiley.com/doi/10.1111/prd.12551 by Universitat Bern, Wiley Online Library on [08/02/2024]. See the Terms and Conditions (https://onlinelibrary.wiley.com/terms-and-conditions) on Wiley Online Library for rules of use; OA articles are governed by the applicable Creative Commons License

grafted with FDBA. The amounts of residual grafting particles of DBBM and FDBA were smaller than the amount of FDBA sintered at higher temperature, which were clearly identified in the entire extraction socket. In the FDBA sintered at higher temperature and DBBM groups, convex alveolar ridges were observed without severe alveolar ridge resorption or dimensions (Figure 8). Fifty-two weeks after surgery, the enhanced radiographic opacity of newly formed bone, reflecting bone maturation, was observed in all groups. The border between the newly formed bone and the DBBM or FDBA particles was poorly identified. In contrast, FDBA sintered at higher temperatures was still clearly detected in all extraction sockets. Concave alveolar ridges with reduced height were detected in six, three, three, two, one, and one of six sites in the sham, DBBA, FDBA, and FDBA sintered at 700°C for 4 h, 900°C for 1 h, and 900°C for 4 h groups, respectively. However, thick and convex alveolar ridges with preserved bone width and height were observed in the rest of the sites (Figure 9).

7.2 | Histological findings at 16 weeks

The alveolar bone in the coronal portion of the buccal area had an irregular outline and was predominated by woven bone, gingival connective tissue or residual bone graft particles to varying degrees, and new bone formation was generally observed from the host bone at the apical and lingual sites in all treatment groups (Figure 10). Immature woven bone and islands of loose trabecular bone were observed in all six nongrafted (blood clot alone) extraction sockets (Figure 10A). Osteoblasts and osteoclasts were observed lining the osteoid covering on the surface of the woven bone, surrounded by yellow bone marrow (Figures 10A and 11A,I). In the DBBM- and FDBA-grafted sites, woven bone was thicker and denser than that in the nongrafted group (Figure 10B,C). The particles of DBBM and FDBA were detected in all extraction sockets, and Howship lacunae were observed on the periphery of the bone grafts, indicating continuing bone graft resorption (Figure 11B,C,J,K). DBBM particles were partially or completely embedded in new mineralized tissue, especially in the center area. The newly formed bone was separated by fibrous connective tissue and bone marrow (Figures 10B and 11B,J). Extraction socket healing at the sites grafted with FDBA was composed of more mature lamellar bone with residual graft particles. Additionally, infiltration of blood vessels was prominent with less fibrous connective tissue compared to the DBBM group (Figures 10C and 11C,K). In the sites that received FDBA sintered at 700°C for 4 h, 900°C for 1 h, 900°C for 4 h, 1300°C for 1 h, and 1300°C for 4 h, a larger number of grafting materials were observed when compared to the DBBM- and FDBA-grafted sites. New bone apposition was generally observed in these groups to varying degrees (Figure 10D–H). Particularly in the groups that received FDBA sintered at 700°C for 4 h and 900°C for 1 h, irregular trabecular bone was formed in the coronal portion of the defects (Figure 10D,E). However, the particles in the center of the defects were in contact with mineralized bone. Patterns of resorption by osteoclasts such as the Howship lacunae were observed at some edges of residual granules of the FDBA sintered at 700°C for 4 h (Figure 11D,L). More blood vessels

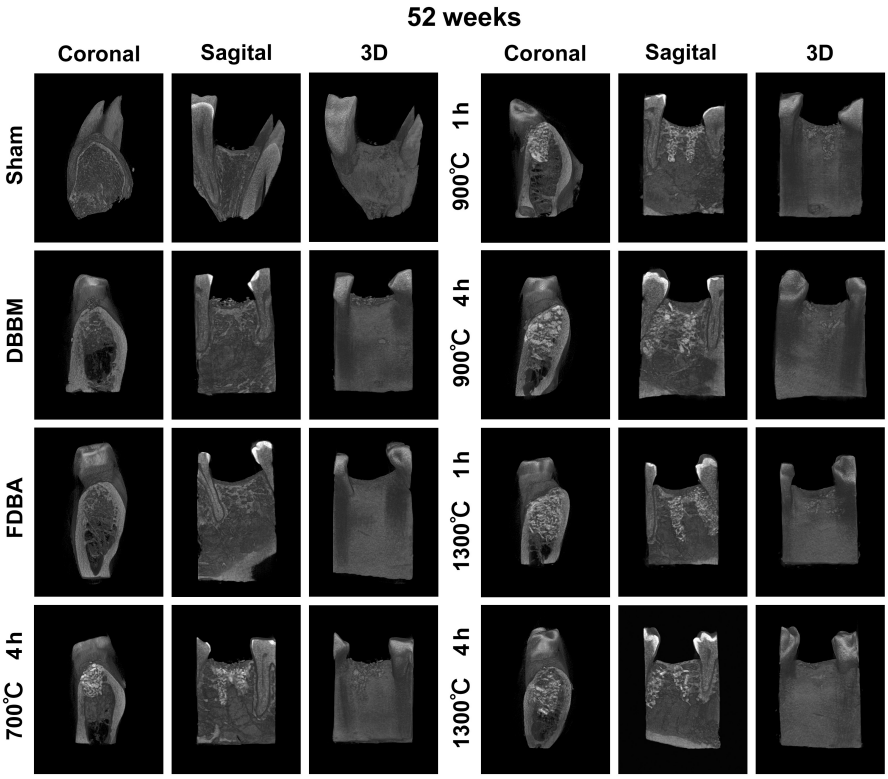

FIGURE 9 Micro-CT images of the extraction sockets in monkeys at 52 weeks. Note the number of large particles left even at 52 weeks postimplantation for allografts sintered at high temperatures.

16000757, 0, Downloaded from https://onlinelibrary.wiley.com/doi/10.1111/prd.12551 by Universitat Bern, Wiley Online Library on [08/02/2024]. See the Terms and Conditions (https://onlinelibrary.wiley.com/terms-and-conditions) on Wiley Online Library for rules of use; OA articles are governed by the applicable Creative Commons License

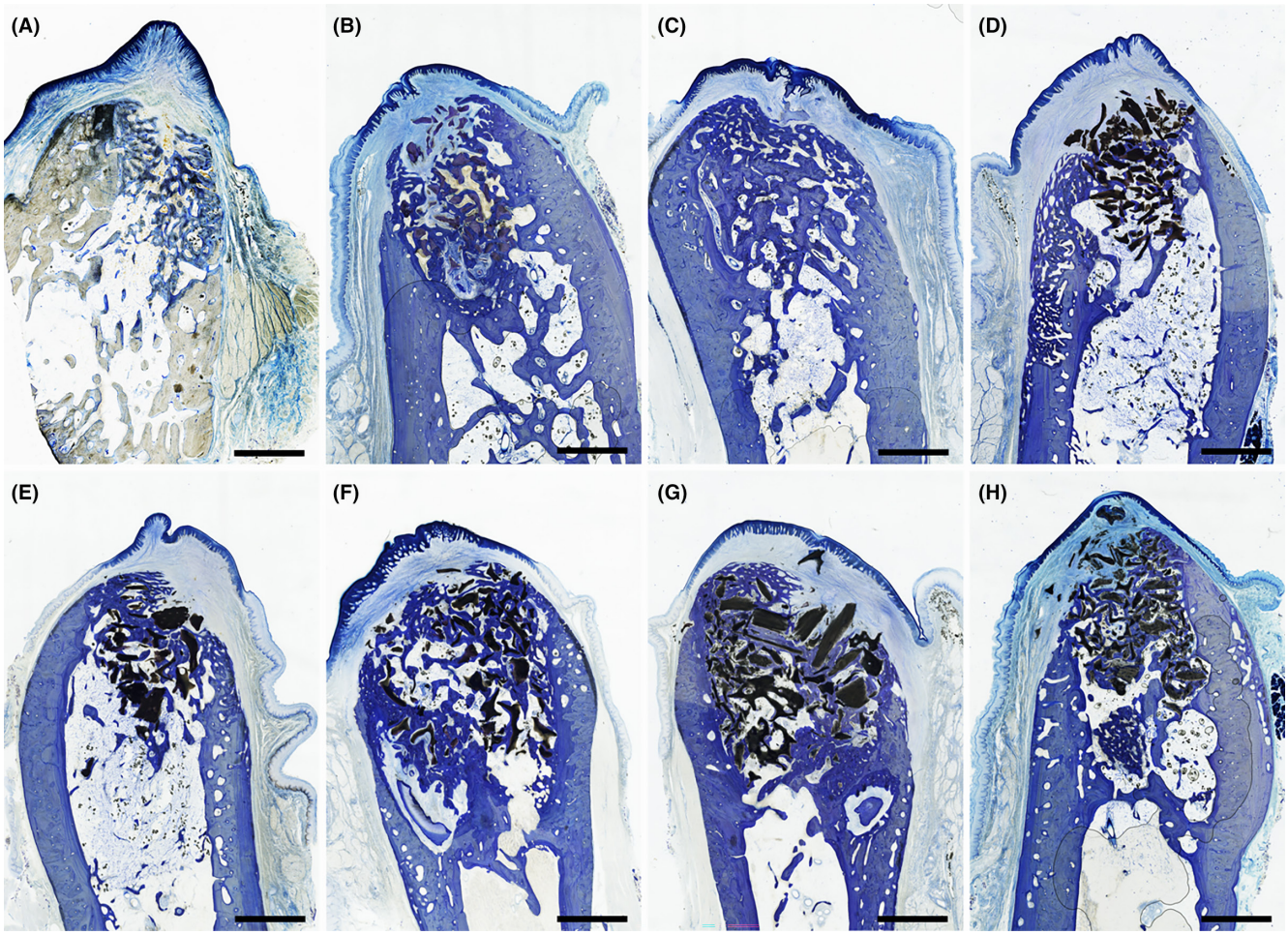

FIGURE 10 Overview photomicrographs of extraction sockets in different groups at 16 weeks (Scale bar, 2 mm, toluidine blue staining, original magnification ×4). (A) Blood clot alone. (B) DBBM. (C) FDBA. (D) FDBA sintered at 700°C for 4 h. (E) FDBA sintered at 900°C for 1 h. (F) FDBA sintered at 900°C for 4 h. (G) FDBA sintered at 1300°C for 1 h and (H) FDBA sintered at 1300°C for 4 h. In total, six sockets per group were investigated utilizing eight total animals (four animals at 16 weeks and another four at 52 weeks).

were detected in the newly formed bone in the FDBA sintered at 900°C for 1 h grafted sites than in the FDBA sintered at 700°C for 4 h (Figure 11D,E,L,M). In the groups grafted with FDBA sintered at 900°C for 4 h, 1300°C for 1 h, and 1300°C for 4 h, various sizes of bone grafting particles were found throughout the extraction socket, maintaining their different polygonal forms and relatively smooth surfaces without large osteoclastic lacunae, and they were intimately associated with the newly formed bone (Figures 10F–H and 11F–H,N–P).

7.3 | Histological findings after 1 year (52 weeks)

Healing within the extraction sockets matured by 52 weeks in all groups. The newly formed bone sealed the extraction socket entrance and bridged across the buccal and lingual/palatal cortical plates in all samples (Figure 12). In the nongrafted group, finger-like bone trabeculae were observed within the extraction socket. Fragments of woven bone associated with a fibrovascular marrow area were present adjacent to fragments of trabecular bone (Figures 12A and 13A,I). Although the continuity of the buccal bone outline was confirmed, the bone-marrow space had enlarged compared with that observed at 16 weeks (Figures 10A and 12A). In the DBBM group, residual particles were rarely seen in 2 sites. In the remaining 4 sites, the DBBM particles were surrounded by mature lamellar bone, although the number of residual small particles decreased compared to that observed at 16 weeks (Figures 12B and 13B,J). Additionally, the bone marrow area decreased with the infiltration of blood vessels in the group (Figures 12B and 13B). Similar to the DBBM group, FDBA particles were hardly observed in 2 sites, and newly formed bone was well integrated with residual bone grafts in 4 sites in the FDBA group (Figures 12C and 13C,K). However, the total area of new bone formation in the extraction sockets was smaller than that at 16 weeks. In the groups that received FDBA sintered at 700°C for 4 h, 900°C for 1 h, 900°C for 4 h, 1300°C for 1 h, and 1300°C for 4 h, bone grafting particles were still clearly observed in all extraction sockets (six sites for each group; Figure 12D–H). Although slight bone graft resorption featuring the Howship lacunae on the

16000757, 0, Downloaded from https://onlinelibrary.wiley.com/doi/10.1111/prd.12551 by Universitat Bern, Wiley Online Library on [08/02/2024]. See the Terms and Conditions (https://onlinelibrary.wiley.com/terms-and-conditions) on Wiley Online Library for rules of use; OA articles are governed by the applicable Creative Commons License

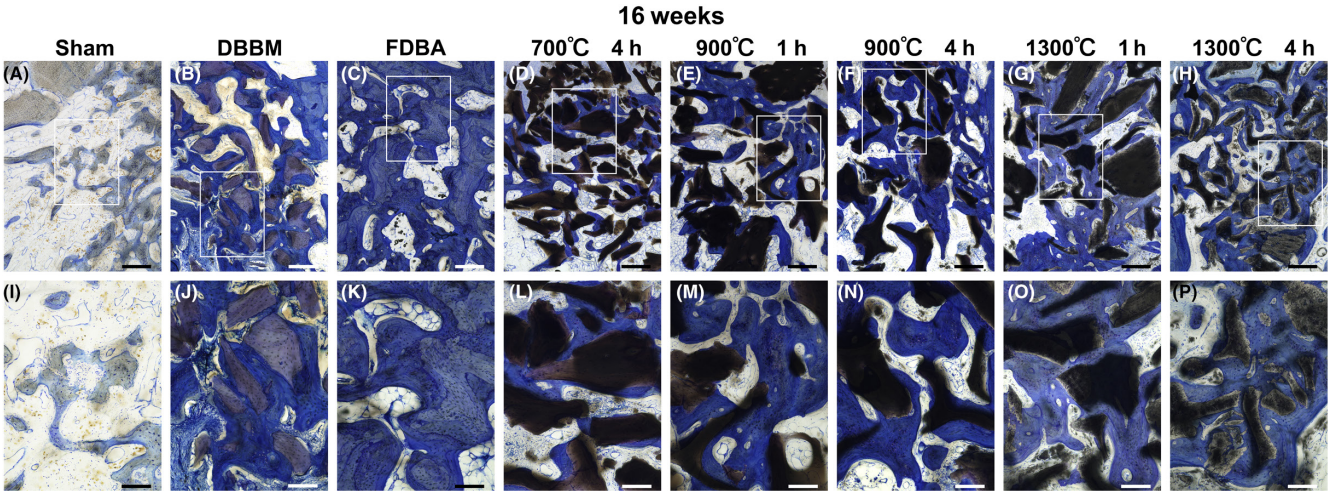

FIGURE 11 Higher magnification of the middle areas in Figure 10. (A) Blood clot alone. (B) DBBM. (C) FDBA. (D) FDBA sintered at 700°C for 4 h. (E) FDBA sintered at 900°C for 1 h. (F) FDBA sintered at 900°C for 4 h. (G) FDBA sintered at 1300°C for 1 h. (H) FDBA sintered at 1300°C for 4 h (scale bar, 400 μm, toluidine blue staining, original magnification ×10). Higher magnification of the framed area in A–H. (I) Blood clot alone. (J) DBBM. (K) FDBA. (L) FDBA sintered at 700°C for 4 h. (M) FDBA sintered at 900°C for 1 h. (N) FDBA sintered at 900°C for 4 h. (O) FDBA sintered at 1300°C for 1 h and (P) FDBA sintered at 1300°C for 4 h (scale bar, 200 μm, toluidine blue staining, original magnification ×40).

surfaces of the FDBA sintered at 700°C for 4 h, 900°C for 1 h, and 900°C for 4 h was observed (Figure 13D–F,L–N), bone-forming activity was prominent in these groups, and newly formed bone areas were larger than those observed at 16 weeks. Healing at FDBA sintered at 900°C for 1 h, 900°C for 4 h, 1300°C for 1 h, and 1300°C for 4 h grafted sites was characterized by the formation of thick bony trabeculae extending from the buccal and lingual cortical plates into the extraction sockets (Figure 12E–H). The areas of newly formed bone in these groups, including many blood vessels and numerous osteocytes, became larger compared to those at 16 weeks of observation. No gaps were observed at the bone-grafting particle interface, and dense newly formed bone was always in close contact with the particles (Figures 13F–H,N–P). In particular, in the sites grafted with FDBA sintered at 1300°C for 1 h and 1300°C for 4 h, newly formed bone was totally integrated with residual bone grafts without resorption of the materials, and new bone could be detected throughout the different levels of the extraction sockets (Figures 10 and 13G,H,P). No apparent differences in healing patterns were detected among the groups. These outcomes obtained in an in vivo preclinical study demonstrated that allografts sintered at high temperatures (greater than 900°C) are highly biocompatible nonresorbable grafting materials for optimizing long-term bone augmentation procedures.

8 | CREATION OF A NONRESORBABLE BONE ALLOGRAFT

Clinicians have raised a significant inquiry to bone-graft companies and manufacturing entities, namely: "Is it not feasible to consolidate our customary ratios, such as a 1:1 proportion of allografts and xenografts, into a singular unit package tailored to specific clinical indications like sinus grafting?" This ability to do so would effectively prevent clinicians from having to purchase two distinct bone-grafting materials, resulting in cost savings. Additionally, it would significantly streamline the procedure and selection of biomaterials, particularly for general practitioners who may not possess the same level of expertise as practicing periodontists and oral surgeons.

Unfortunately, owing to regulatory and government bodies, it is not possible to premix biomaterials from two different donors (such as an allograft from a human and a xenograft from a cow). Should the graft be contaminated, too many regulatory questions/concerns would arise regarding whether the former or the latter was the cause. Accordingly, for decades, clinicians have incorporated dual bone grafts into many procedures.

9 | OPTIMIZED BONE GRAFTING: INTRODUCING NONRESORBABLE BONE ALLOGRAFTS (NRBAS)

Because of these regulatory guidelines, our research group sought to process standard bone allografts in the same sintering conditions/environment as xenografts. Thus, our research group has developed NRBAs produced at various temperatures ranging from 300 to 1400°C for 1–8 h.[102] Following this development, a 52-week monkey study also demonstrated the ability of the grafts to remain integrated into bone without fear of resorption, displaying maintained ridges with bone grafting particles even after 52 weeks as confirmed by CBCT and histological analysis. Thus, it is possible to recreate the biological/mechanical properties of xenografts utilizing sintered allograft bone.

16000757, 0, Downloaded from https://onlinelibrary.wiley.com/doi/10.1111/prd.12551 by Universitat Bern, Wiley Online Library on [08/02/2024]. See the Terms and Conditions (https://onlinelibrary.wiley.com/terms-and-conditions) on Wiley Online Library for rules of use; OA articles are governed by the applicable Creative Commons License

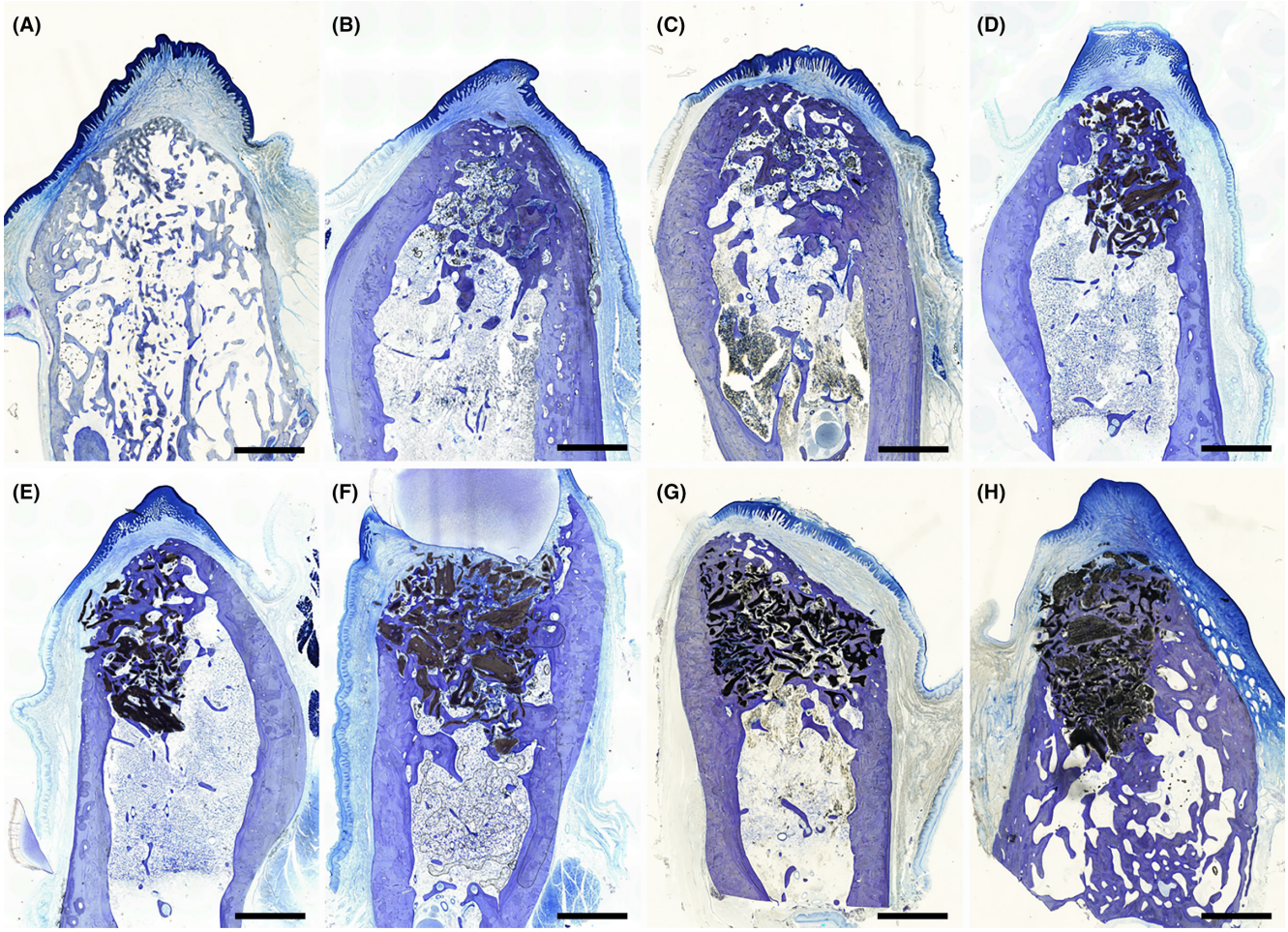

FIGURE 12 Overview photomicrographs of extraction sockets in different groups at 52 weeks (scale bar, 2 mm, toluidine blue staining, magnification ×4). (A) Blood clot alone. (B) DBBM. (C) FDBA. (D) FDBA sintered at 700°C for 4 h. (E) FDBA sintered at 900°C for 1 h. (F) FDBA sintered at 900°C for 4 h. (G) FDBA sintered at 1300°C for 1 h and (H) FDBA sintered at 1300°C for 4 h. In total, 6 sockets per group were investigated utilizing eight total animals (four animals at 16 weeks and another four at 52 weeks). In total, six sockets per group were investigated utilizing eight total animals (four animals at 16 weeks and another four at 52 weeks).

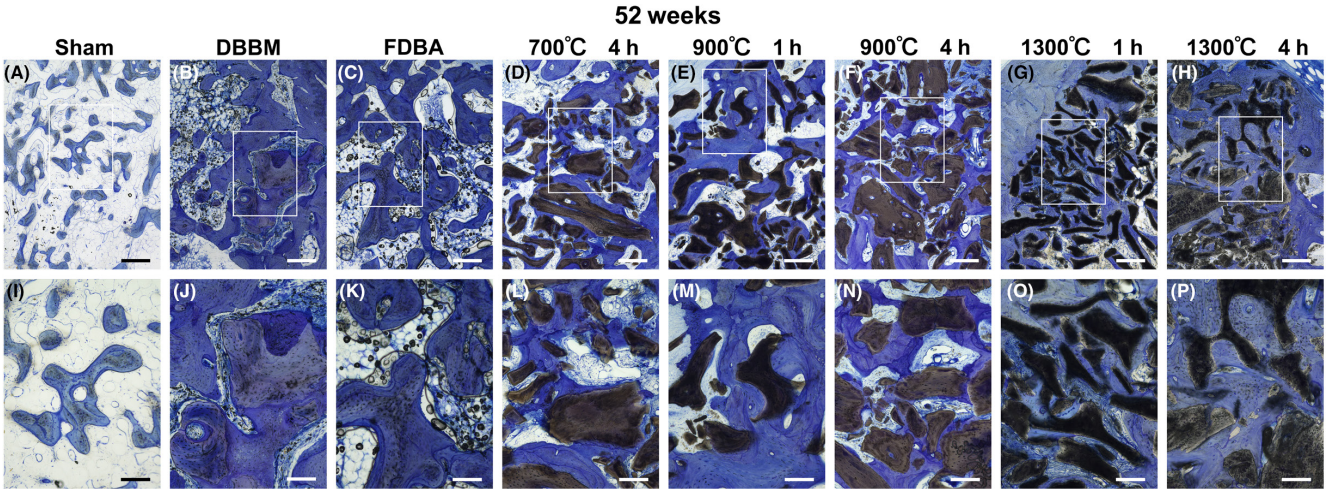

FIGURE 13 Higher magnification of the middle area in Figure 12. (A) Blood clot alone. (B) DBBM. (C) FDBA. (D) FDBA sintered at 700° for 4 h. (E) FDBA sintered at 900°C for 1 h. (F) FDBA sintered at 900°C for 4 h. (G) FDBA sintered at 1300°C for 1 h. (H) FDBA sintered at 1300°C for 4 h (scale bar, 400 μm, toluidine blue staining, original magnification ×10) and higher magnification of the framed area in (A–H). (I) Blood clot alone. (J) DBBM. (K) FDBA. (L) FDBA sintered at 700°C for 4 h. (M) FDBA sintered at 900°C for 1 h. (N) FDBA sintered at 900°C for 4 h. (O) FDBA sintered at 1300°C for 1 h and (P) FDBA sintered at 1300°C for 4 h (scale bar, 200 μm, toluidine blue staining, original magnification ×40).

16000757, 0, Downloaded from https://onlinelibrary.wiley.com/doi/10.1111/prd.12551 by Universitat Bern, Wiley Online Library on [08/02/2024]. See the Terms and Conditions (https://onlinelibrary.wiley.com/terms-and-conditions) on Wiley Online Library for rules of use; OA articles are governed by the applicable Creative Commons License

TABLE 3 Various clinical grafting procedures and the ability to pre-mix FDBA, DFDBA and non-resorbable bone allografts (NRBAs) in various ratios.

Grafting Procedures	Historic use of bone grafts	Examples of potential optimized bone grafts	Advantages
Extraction site management	Freeze-dried bone allografts (FDBA)	3:1 ratio of FDBA/ DFDBA	• Maintains ridge owing to its large incorporation of FDBA but possesses an ability to release quickly growth factors responsible for bone formation in DFDBA • 25% DFDBA with an ability to "kick start" the bone regeneration process
Intrabony/Furcation defects 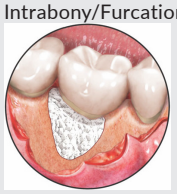	Demineralized freeze-dried bone allograft (DFDBA)	3:1 ratio of DFDBA/ FDBA	• Faster ability to release growth factors necessary for periodontal regeneration owing to demineralization process of DFDBA • 25% of the graft remains FDBA to hold volume slightly better than pure DFDBA
Contour augmentation 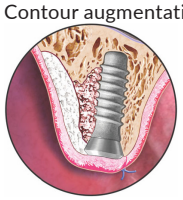	Non-resorbable xenograft: deproteinized bovine bone mineral (DBBM)	3:1 ratio of non-resorbable bone allograft (NRBA) with DFDBA	• Non-resorbable bone allograft (NRBA) acts like a xenograft yet more biocompatible owing to its human base source • 25% of the graft is DFDBA to dramatically "kick start" the bone regeneration process when compared to pure xenografts
Sinus grafting 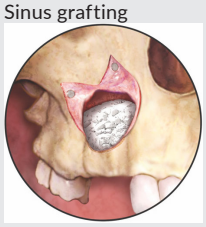	*1:1 mixture of*: Freeze-dried bone allografts (FDBA) mixed with non-resorbable xenograft: Deproteinized bovine bone mineral (DBBM)	1:1 ratio of NRBA and FDBA	• Non-resorbable bone allograft can now be premixed with standard FDBA together in a single pre-mixed package • Cheaper costs having to buy only 1 bone graft and faster clinical procedures with less room for error
Guided bone regeneration 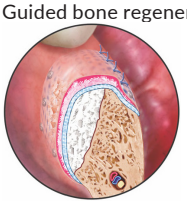	*70:30 mixture of*: Freeze-dried bone allografts (FDBA) mixed with non-resorbable xenograft: Deproteinized bovine bone mineral (DBBM)	3:1 ratio of FDBA and NRBA	• Non-resorbable bone allograft can now be premixed with standard FDBA together in a single pre-mixed package • Cheaper costs having to buy only 1 bone graft and faster clinical procedures with less room for error

10 | CONCEPTUALIZATION OF PREMIXING VARIOUS COMBINATIONS OF ALLOGRAFTS AND NONRESORBABLE ALLOGRAFTS FOR SIMPLIFIED AND OPTIMIZED BONE GRAFTING

The development of NRBAs has facilitated the production of xenograft/allograft premixes, whereby NRBAs and allografts derived from the same donor may be combined. Therefore, clinicians have the option to access a range of premixed bone grafts based on their specific clinical indications, as shown in Table 3. The benefits of these grafts, particularly in terms of their combinations, are emphasized. These preformulated bone grafts, intentionally formulated in different proportions, can significantly enhance the ability of clinicians to carry out grafting procedures highlighted in the literature based on the utilization of various biomaterials supported by evidence. Additionally, they streamline and optimize the described techniques by reducing the need to purchase multiple bone grafts, as only one is needed. Additional study is required to ascertain the optimal combinations and ratios for each therapeutic condition. However, the objective of this study is to streamline the selection of grafting materials for clinicians that prefer pre-fabricated mixes through development of NRBAs.

With the development of NRBAs, it has recently been possible to manufacture a combination of xenograft/allograft premixes by utilizing NRBA/allograft mixes coming from the same donor. Thus, a variety of premixed bone grafts for different clinical indications can be made available to clinicians, as presented in Table 3, with advantages highlighted regarding their combinations. These premixed bone grafts purposefully designed in various ratios can better enable the treating clinician not only to perform highlighted grafting procedures following the evidence-based use of various biomaterials but also to simplify and optimize the described techniques by

16000757, 0, Downloaded from https://onlinelibrary.wiley.com/doi/10.1111/prd.12551 by Universitat Bern, Wiley Online Library on [08/02/2024]. See the Terms and Conditions (https://onlinelibrary.wiley.com/terms-and-conditions) on Wiley Online Library for rules of use; OA articles are governed by the applicable Creative Commons License

requiring the purchase of one bone graft as opposed to multiple. Naturally, much additional research is needed to determine which combinations and ratios are best for each clinical indication, but the proposed work aims to simplify grafting material choices by clinicians seeking more predictable bone grafting owing to the recent development of NRBAs.

ACKNOWLEDGMENTS

Not applicable for personnel. This paper is in agreement with the guidelines of the Helsinki Declaration, as revised in 1975. Open access funding provided by Universitat Bern.

CONFLICT OF INTEREST STATEMENT

Not applicable.

DATA AVAILABILITY STATEMENT

Data available on request from the authors.

ORCID

Yufeng Zhang https://orcid.org/0000-0001-8702-5291
Yoshinori Shirakata https://orcid.org/0000-0003-0663-0524

REFERENCES

1. Jung RE, Fenner N, Hammerle CH, Zitzmann NU. Long-term outcome of implants placed with guided bone regeneration (GBR) using resorbable and non-resorbable membranes after 12-14 years. *Clin Oral Implants Res*. 2013;24:1065-1073.
2. Dahlin C, Linde A, Gottlow J, Nyman S. Healing of bone defects by guided tissue regeneration. *Plast Reconstr Surg*. 1988;81:672-676.
3. Buser D, Dula K, Belser U, Hirt HP, Berthold H. Localized ridge augmentation using guided bone regeneration. 1. Surgical procedure in the maxilla. *Int J Periodontics Restorative Dent*. 1993;13:29-45.
4. Buser D, Dahlin C, Schenk R. *Guided Bone Regeneration*. Quintessence; 1994.
5. Hardwick R, Dahlin C. Healing pattern of bone regeneration in membrane-protected defects: a histologic study in the canine mandible. *Int J Oral Maxillofac Implants*. 1994;9:13-29.
6. Miron RJ, Sculean A, Shuang Y, et al. Osteoinductive potential of a novel biphasic calcium phosphate bone graft in comparison with autographs, xenografts, and DFDBA. *Clin Oral Implants Res*. 2016;27:668-675.
7. Miron RJ. Optimized bone grafting. *Periodontol 2000*. doi:10.1111/prd.12517
8. Sanz M, Vignoletti F. Key aspects on the use of bone substitutes for bone regeneration of edentulous ridges. *Dent Mater*. 2015;31:640-647.
9. Jensen SS, Gruber R, Buser D, Bosshardt DD. Osteoclast-like cells on deproteinized bovine bone mineral and biphasic calcium phosphate: light and transmission electron microscopical observations. *Clin Oral Implants Res*. 2015;26:859-864.
10. Pikos MA, Miron RJ. *Bone Augmentation in Implant Dentistry*. Quintessence Publishing; 2019.
11. Miron RJ, Zhang Y. *Next-Generation Biomaterials for Bone & Periodontal Regeneration*. Quintessence Publishing Company, Incorporated; 2019.
12. Gonçalves D, Thompson TJ, Cunha E. Implications of heat-induced changes in bone on the interpretation of funerary behaviour and practice. *J Archaeol Sci*. 2011;38:1308-1313.
13. Thompson T. Recent advances in the study of burned bone and their implications for forensic anthropology. *Forensic Sci Int*. 2004;146:S203-S205.
14. Ubelaker DH. The forensic evaluation of burned skeletal remains: a synthesis. *Forensic Sci Int*. 2009;183:1-5.
15. Shipman P, Foster G, Schoeninger M. Burnt bones and teeth: an experimental study of color, morphology, crystal structure and shrinkage. *J Archaeol Sci*. 1984;11:307-325.
16. Ellingham ST, Thompson TJ, Islam M, Taylor G. Estimating temperature exposure of burnt bone—a methodological review. *Sci Justice*. 2015;55:181-188.
17. Bohnert M, Rost T, Pollak S. The degree of destruction of human bodies in relation to the duration of the fire. *Forensic Sci Int*. 1998;95:11-21.
18. Figueiredo M, Fernando A, Martins G, Freitas J, Judas F, Figueiredo H. Effect of the calcination temperature on the composition and microstructure of hydroxyapatite derived from human and animal bone. *Ceram Int*. 2010;36:2383-2393.
19. Mkukuma L, Skakle JMS, Gibson IR, Imrie CT, Aspden RM, Hukins DWL. Effect of the proportion of organic material in bone on thermal decomposition of bone mineral: an investigation of a variety of bones from different species using thermogravimetric analysis coupled to mass spectrometry, high-temperature X-ray diffraction, and Fourier transform infrared spectroscopy. *Calcif Tissue Int*. 2004;75:321-328.
20. Peters F, Schwarz K, Epple M. The structure of bone studied with synchrotron X-ray diffraction, X-ray absorption spectroscopy and thermal analysis. *Thermochim Acta*. 2000;361:131-138.
21. Correia PM. Fire modification of bone: a review of the literature. In: Haglund WD, Sorg MH, eds. *Forensic Taphonomy: The Postmortem Fate of Human Remains*. CRC Press; 1997:275-293.
22. Pramanik S, Hanif ASM, Pingguan-Murphy B, Abu Osman NA. Morphological change of heat treated bovine bone: a comparative study. *Materials*. 2012;6:65-75.
23. Ellingham ST, Thompson TJ, Islam M. The effect of soft tissue on temperature estimation from burnt bone using Fourier transform infrared spectroscopy. *J Forensic Sci*. 2016;61:153-159.
24. Ellingham S, Thompson T, Islam M. Thermogravimetric analysis of property changes and weight loss in incinerated bone. *Palaeogeogr Palaeoclimatol Palaeoecol*. 2015;438:239-244.
25. Chen P-Y, Toroian D, Price PA, McKittrick J. Minerals form a continuum phase in mature cancellous bone. *Calcif Tissue Int*. 2011;88:351-361.
26. Rho J-Y, Kuhn-Spearing L, Zioupos P. Mechanical properties and the hierarchical structure of bone. *Med Eng Phys*. 1998;20:92-102.
27. Olszta MJ, Cheng X, Jee SS, et al. Bone structure and formation: a new perspective. *Mater Sci Eng R Rep*. 2007;58:77-116.
28. Bohner M. Calcium orthophosphates in medicine: from ceramics to calcium phosphate cements. *Injury*. 2000;31:D37-D47.
29. Bohner M. Bioresorbable ceramics. In: Buchanan FJ, ed. *Degradation Rate of Bioresorbable Materials*. Elsevier; 2008:95-114.
30. Elliott JC. *Structure and Chemistry of the Apatites and Other Calcium Orthophosphates*. Elsevier; 2013.
31. LeGeros R. Calcium phosphate materials in restorative dentistry: a review. *Adv Dent Res*. 1988;2:164-180.
32. Benard J. *Combinaisons avec le phosphore Nouveau trait6 de chimieminerale*. Vol 4. Masson; 1958:455-488.
33. Eggli P, Moller W, Schenk R. Porous hydroxyapatite and tricalcium phosphate cylinders with two different pore size ranges implanted in the cancellous bone of rabbits: a comparative histomorphometric and histologic study of bony ingrowth and implant substitution. *Clin Orthop Relat Res*. 1988;232:127-138.
34. Welch J, Gutt W. 874. High-temperature studies of the system calcium oxide–phosphorus pentoxide. *J Chem Soc*. 1961;0:4442-4444.

16000757, 0, Downloaded from https://onlinelibrary.wiley.com/doi/10.1111/prd.12551 by Universitat Bern, Wiley Online Library on [08/02/2024]. See the Terms and Conditions (https://onlinelibrary.wiley.com/terms-and-conditions) on Wiley Online Library for rules of use; OA articles are governed by the applicable Creative Commons License

35. Mortier A, Lemaitre J, Rodrique L, Rouxhet PG. Synthesis and thermal behavior of well-crystallized calcium-deficient phosphate apatite. *J Solid State Chem*. 1989;78:215-219.
36. Mortier A, Lemaitre J, Rouxhet PG. Temperature-programmed characterization of synthetic calcium-deficient phosphate apatites. *Thermochim Acta*. 1989;143:265-282.
37. Kanazawa T. *Inorganic Phosphate Materials. Materials Science Monographs*. Elsevier; 1989:52.
38. Riboud PV. *Composition et stabilité des phases a structure d'apatie dans le système CaO-P2O5-oxyde de fer-H20 à haute température*. Masson & Cie; 1973.
39. Gisep A, Wieling R, Bohner M, Matter S, Schneider E, Rahn B. Resorption patterns of calcium-phosphate cements in bone. *J Biomed Mater Res A*. 2003;66:532-540.
40. Oonishi H, Hench L, Wilson J, et al. Comparative bone growth behavior in granules of bioceramic materials of various sizes. *J Biomed Mater Res*. 1999;44:31-43.
41. Flautre B, Ikenaga M, Andrianjatovo H, et al. Evaluation des propriétés biologiques in vivo chez le lapin d'un ciment hydraulique phospho-calcique. 1998.
42. Linhart W, Briem D, Amling M, Rueger J, Windolf J. Mechanical failure of porous hydroxyapatite ceramics 7.5 years after implantation in the proximal tibial. *Unfallchirurg*. 2004;107:154-157.
43. Bohner M. Resorbable biomaterials as bone graft substitutes. *Mater Today*. 2010;13:24-30.
44. LeGeros RZ. Biodegradation and bioresorption of calcium phosphate ceramics. *Clin Mater*. 1993;14:65-88.
45. LeGeros R, Parsons JR, Daculsi G, et al. Significance of the porosity and physical chemistry of calcium phosphate ceramics biodegradation-bioresorption. *Ann N Y Acad Sci*. 1988;523:268-271.
46. Chang B-S, Hong K-S, Youn H-J, Ryu H-S, Chung S-S, Park K-W. Osteoconduction at porous hydroxyapatite with various pore configurations. *Biomaterials*. 2000;21:1291-1298.
47. Chu T-MG, Orton DG, Hollister SJ, Feinberg SE, Halloran JW. Mechanical and in vivo performance of hydroxyapatite implants with controlled architectures. *Biomaterials*. 2002;23:1283-1293.
48. Gauthier O, Bouler J-M, Aguado E, Pilet P, Daculsi G. Macroporous biphasic calcium phosphate ceramics: influence of macropore diameter and macroporosity percentage on bone ingrowth. *Biomaterials*. 1998;19:133-139.
49. Lu J, Flautre B, Anselme K, et al. Role of interconnections in porous bioceramics on bone recolonization in vitro and in vivo. *J Mater Sci Mater Med*. 1999;10:111-120.
50. Lu J, Gallur A, Flautre B, et al. Comparative study of tissue reactions to calcium phosphate ceramics among cancellous, cortical, and medullar bone sites in rabbits. *J Biomed Mater Res*. 1998;42:357-367.
51. Malard O, Bouler JM, Guicheux J, et al. Influence of biphasic calcium phosphate granulometry on bone ingrowth, ceramic resorption, and inflammatory reactions: preliminary in vitro and in vivo study. *J Biomed Mater Res*. 1999;46:103-111.
52. Berger G, Gildenhaar R, Ploska U, Driessens F, Planell J. Short-term dissolution behaviour of some calcium phosphate cements and ceramics. *J Mater Sci Lett*. 1997;16:1267-1269.
53. Chow LC, Markovic M, Takagi S. A dual constant-composition titration system as an in vitro resorption model for comparing dissolution rates of calcium phosphate biomaterials. *J Biomed Mater Res*. 2003;65:245-251.
54. Ducheyne P, Radin S, King L. The effect of calcium phosphate ceramic composition and structure on in vitro behavior. I. Dissolution. *J Biomed Mater Res*. 1993;27:25-34.
55. Fulmer MT, Ison IC, Hankermayer CR, Constantz BR, Ross J. Measurements of the solubilities and dissolution rates of several hydroxyapatites. *Biomaterials*. 2002;23:751-755.
56. LeGeros RZ. Properties of osteoconductive biomaterials: calcium phosphates. *Clin Orthop Relat Res*. 2002;395:81-98.
57. Alam MI, Asahina I, Ohmamiuda K, Takahashi K, Yokota S, Enomoto S. Evaluation of ceramics composed of different hydroxyapatite to tricalcium phosphate ratios as carriers for rhBMP-2. *Biomaterials*. 2001;22:1643-1651.
58. Koerten H, Van der Meulen J. Degradation of calcium phosphate ceramics. *J Biomed Mater Res*. 1999;44:78-86.
59. Neo M, Kotani S, Fujita Y, et al. Differences in ceramic–bone interface between surface-active ceramics and resorbable ceramics: a study by scanning and transmission electron microscopy. *J Biomed Mater Res*. 1992;26:255-267.
60. Fujita Y, Yamamuro T, Nakamura T, Kotani S, Ohtsuki C, Kokubo T. The bonding behavior of calcite to bone. *J Biomed Mater Res*. 1991;25:991-1003.
61. Dreesmann H. Ueber Knochenplombirung1. *Dtsch Med Wochenschr*. 1893;19:445-446.
62. Flautre B, Delecourt C, Blary M-C, Van Landuyt P, Lemaî tre J, Hardouin P. Volume effect on biological properties of a calcium phosphate hydraulic cement: experimental study in sheep. *Bone*. 1999;25:35S-39S.
63. Stubbs D, Deakin M, Chapman-Sheath P, et al. In vivo evaluation of resorbable bone graft substitutes in a rabbit tibial defect model. *Biomaterials*. 2004;25:5037-5044.
64. Ducheyne P, Lemons JE. Bioceramics: Material Characteristics Versus In Vivo Behavior. 1988.
65. Driessens F, Verbeeck R. The dynamics of bone mineral in some vertebrates. *Z Naturforsch C J Biosci*. 1986;41:468-471.
66. Driessens F, Verbeeck R. Relation between physico-chemical solubility and biodegradability of calcium phosphates. *Implant Materials in Biofunction, Advances in Biomaterials*. Elsevier; 1988:105-111.
67. Driessens F. The mineral in bone, dentin and tooth enamel. *Bull Soc Chim Belg*. 1980;89:663-689.
68. Fricain J, Bareille R, Ulysse F, Dupuy B, Amedee J. Evaluation of proliferation and protein expression of human bone marrow cells cultured on coral crystallized in the aragonite or calcite form. *J Biomed Mater Res*. 1998;42:96-102.
69. Ota Y, Iwashita T, Kasuga T, Abe Y, Seki A. Bone formation following implantation of fibrous calcium compounds (β− Ca (PO 3) 2, CaCO 3 (aragonite)) into bone marrow. *J Mater Sci Mater Med*. 2002;13:895-900.
70. Wu C, Chang J, Wang J, Ni S, Zhai W. Preparation and characteristics of a calcium magnesium silicate (bredigite) bioactive ceramic. *Biomaterials*. 2005;26:2925-2931.
71. Wu C, Chang J, Zhai W, Ni S. A novel bioactive porous bredigite (Ca 7 MgSi 4 O 16) scaffold with biomimetic apatite layer for bone tissue engineering. *J Mater Sci Mater Med*. 2007;18:857-864.
72. Nelson SR, Wolford LM, Lagow RJ, Capano PJ, Davis WL. Evaluation of new high-performance calcium polyphosphate bioceramics as bone graft materials. *J Oral Maxillofac Surg*. 1993;51:1363-1371.
73. Baksh D, Davies J, Kim S. Three-dimensional matrices of calcium polyphosphates support bone growth in vitro and in vivo. *J Mater Sci Mater Med*. 1998;9:743-748.
74. Grynpas M, Pilliar R, Kandel R, Renlund R, Filiaggi M, Dumitriu M. Porous calcium polyphosphate scaffolds for bone substitute applications in vivo studies. *Biomaterials*. 2002;23:2063-2070.
75. Lee YM, Seol YJ, Lim YT, et al. Tissue-engineered growth of bone by marrow cell transplantation using porous calcium metaphosphate matrices. *J Biomed Mater Res*. 2001;54:216-223.
76. Knabe C, Driessens F, Planell J, et al. Evaluation of calcium phosphates and experimental calcium phosphate bone cements using osteogenic cultures. *J Biomed Mater Res*. 2000;52:498-508.

16000757, 0, Downloaded from https://onlinelibrary.wiley.com/doi/10.1111/prd.12551 by Universitat Bern, Wiley Online Library on [08/02/2024]. See the Terms and Conditions (https://onlinelibrary.wiley.com/terms-and-conditions) on Wiley Online Library for rules of use; OA articles are governed by the applicable Creative Commons License

77. Lin F-H, Liao C-J, Chen K-S, Sun J-S. Preparation of a biphasic porous bioceramic by heating bovine cancellous bone with Na4P2O7·10H2O addition. *Biomaterials*. 1999;20:475-484.
78. Sun JS, Huang YC, Tsuang YH, Chen LT, Lin FH. Sintered dicalcium pyrophosphate increases bone mass in ovariectomized rats. *J Biomed Mater Res*. 2002;59:246-253.
79. Sun JS, Tsuang YH, Liao CJ, Liu HC, Hang YS, Lin FH. The effect of sintered β-dicalcium pyrophosphate particle size on newborn Wistar rat osteoblasts. *Artif Organs*. 1999;23:331-338.
80. Sun JS, Tsuang YH, Liao CJ, Liu HC, Hang YS, Lin FH. The effects of calcium phosphate particles on the growth of osteoblasts. *J Biomed Mater Res*. 1997;37:324-334.
81. Ni S, Chang J, Chou L. A novel bioactive porous CaSiO3 scaffold for bone tissue engineering. *J Biomed Mater Res A*. 2006;76:196-205.
82. Sarmento C, Luklinska ZB, Brown L, et al. In vitro behavior of osteoblastic cells cultured in the presence of pseudowollastonite ceramic. *J Biomed Mater Res A*. 2004;69:351-358.
83. De Aza P, Guitian F, De Aza S. Bioeutectic: a new ceramic material for human bone replacement. *Biomaterials*. 1997;18:1285-1291.
84. De Aza P, Luklinska Z, Anseau M, Hector M, Guitian F, De Aza S. Reactivity of a wollastonite–tricalcium phosphate bioeutectic® ceramic in human parotid saliva. *Biomaterials*. 2000;21:1735-1741.
85. F. C. M. DRIESSENS. ECERS, Maastricht. 1989.
86. Driessens F, Ramselaar M, Schaeken H, Stols A, Van Mullem P, De Wijn J. Chemical reactions of calcium phosphate implants after implantation in vivo. *J Mater Sci Mater Med*. 1992;3:413-417.
87. Dreesmann H. Knochenplombierung bei Hohlenforigen defekten des Knochens. *Beitr Klin Chir*. 1892;9:804-810.
88. Walsh W, Morberg P, Yu Y, et al. Response of a calcium sulfate bone graft substitute in a confined cancellous defect. *Clin Orthop Relat Res*. 2003;406:228-236.
89. Langstaff S, Sayer M, Smith T, Pugh S, Hesp S, Thompson W. Resorbable bioceramics based on stabilized calcium phosphates. Part I: rational design, sample preparation and material characterization. *Biomaterials*. 1999;20:1727-1741.
90. Sayer M, Stratilatov A, Reid J, et al. Structure and composition of silicon-stabilized tricalcium phosphate. *Biomaterials*. 2003;24:369-382.
91. Gibson I, Best S, Bonfield W. Chemical characterization of silicon-substituted hydroxyapatite. *J Biomed Mater Res*. 1999;44:422-428.
92. Tang R, Nancollas GH, Orme CA. Mechanism of dissolution of sparingly soluble electrolytes. *J Am Chem Soc*. 2001;123:5437-5443.
93. Silver I, Murrills R, Etherington D. Microelectrode studies on the acid microenvironment beneath adherent macrophages and osteoclasts. *Exp Cell Res*. 1988;175:266-276.
94. Vereecke G, Lemaître J. Calculation of the solubility diagrams in the system Ca (OH) 2-H_3PO_4-KOH-HNO_3-CO_2-H_2O. *J Cryst Growth*. 1990;104:820-832.
95. Kamakura S, Sasano Y, Shimizu T, et al. Implanted octacalcium phosphate is more resorbable than β-tricalcium phosphate and hydroxyapatite. *J Biomed Mater Res*. 2002;59:29-34.
96. Barralet J, Akao M, Aoki H, Aoki H. Dissolution of dense carbonate apatite subcutaneously implanted in Wistar rats. *J Biomed Mater Res*. 2000;49:176-182.
97. Bohner M, Theiss F, Apelt D, et al. Compositional changes of a dicalcium phosphate dihydrate cement after implantation in sheep. *Biomaterials*. 2003;24:3463-3474.
98. Kamakura S, Sasano Y, Homma-Ohki H, et al. Multinucleated giant cells recruited by implantation of octacalcium phosphate (OCP) in rat bone marrow share ultrastructural characteristics with osteoclasts. *Microscopy*. 1997;46:397-403.
99. Liu C, Shen W, Chen J. Solution property of calcium phosphate cement hardening body. *Mater Chem Phys*. 1999;58:78-82.
100. Nancollas G. Phase tranformation during precipitation of calcium salts. *Biological Mineralization and Demineralization: Report of the Dahlem Workshop on Biological Mineralization and Demineralization Berlin 1981, October 18–23*. Springer; 1982.
101. Apelt D, Theiss F, El-Warrak A, et al. In vivo behavior of three different injectable hydraulic calcium phosphate cements. *Biomaterials*. 2004;25:1439-1451.
102. Miron RJ. Non-resorbable bone allografts and method for making same: Google Patents. 2020.
103. Turitto V, Slack S. C1. 1 introduction. In: Murphy W, Black J, Hastings G, eds. *Handbook of Biomaterial Properties*. Springer; 1998:114.

How to cite this article: Miron RJ, Fujioka-Kobayashi M, Pikos MA, et al. The development of non-resorbable bone allografts: Biological background and clinical perspectives. *Periodontol 2000*. 2024;00:1-19. doi:10.1111/prd.12551

16000757, 0, Downloaded from https://onlinelibrary.wiley.com/doi/10.1111/prd.12551 by Universitat Bern, Wiley Online Library on [08/02/2024]. See the Terms and Conditions (https://onlinelibrary.wiley.com/terms-and-conditions) on Wiley Online Library for rules of use; OA articles are governed by the applicable Creative Commons License